

Factor-guided estimation of large covariance matrix function with conditional functional sparsity

Dong Li¹, Xinghao Qiao², and Zihan Wang¹

¹*Center for Statistical Science, Tsinghua University, Beijing 100084, China*

²*Department of Statistics, London School of Economics, London WC2A 2AE, U.K.*

Abstract

This paper addresses the fundamental task of estimating covariance matrix functions for high-dimensional functional data/functional time series. We consider two functional factor structures encompassing either functional factors with scalar loadings or scalar factors with functional loadings, and postulate functional sparsity on the covariance of idiosyncratic errors after taking out the common unobserved factors. To facilitate estimation, we rely on the spiked matrix model and its functional generalization, and derive some novel asymptotic identifiability results, based on which we develop DIGIT and FPOET estimators under two functional factor models, respectively. Both estimators involve performing associated eigenanalysis to estimate the covariance of common components, followed by adaptive functional thresholding applied to the residual covariance. We also develop functional information criteria for the purpose of model selection. The convergence rates of estimated factors, loadings, and conditional sparse covariance matrix functions under various functional matrix norms, are respectively established for DIGIT and FPOET estimators. Numerical studies including extensive simulations and two real data applications on mortality rates and functional portfolio allocation are conducted to examine the finite-sample performance of the proposed methodology.

Keywords: Adaptive functional thresholding; Asymptotic identifiability; Eigenanalysis; Functional factor model; High-dimensional functional data/functional time series; Model selection.

1 Introduction

With advancements in data collection technology, multivariate functional data/functional time series are emerging in a wide range of scientific and economic applications. Examples include different types of brain imaging data in neuroscience, intraday return trajectories for a collection of stocks, age-specific mortality rates across different countries, and daily energy consumption curves from thousands of households, among others. Such data can be represented as $\mathbf{y}_t(\cdot) = \{y_{t1}(\cdot), \dots, y_{tp}(\cdot)\}^\top$ defined on a compact interval \mathcal{U} , with the marginal- and cross-covariance operators induced from the associated kernel functions. These operators together form the operator-valued covariance matrix, which is also referred to as the following covariance matrix function for notational simplicity:

$$\boldsymbol{\Sigma}_y = \{\Sigma_{y,jk}(\cdot, \cdot)\}_{p \times p}, \quad \Sigma_{y,jk}(u, v) = \text{Cov}\{y_{tj}(u), y_{tk}(v)\}, \quad (u, v) \in \mathcal{U}^2,$$

and we observe stationary $\mathbf{y}_t(\cdot)$ for $t = 1, \dots, n$.

The estimation of covariance matrix function and its inverse is of paramount importance in multivariate functional data/functional time series analysis. An estimator of $\boldsymbol{\Sigma}_y$ is not only of interest in its own right but also essential for subsequent analyses, such as dimension reduction and modeling of $\{\mathbf{y}_t(\cdot)\}$. Examples include multivariate functional principal components analysis (MFPCA) (Happ and Greven, 2018), functional risk management to account for intraday uncertainties, functional graphical model estimation (Qiao et al., 2019), multivariate functional linear regression (Chiou et al., 2016) and functional linear discriminant analysis (Xue et al., 2023). See Section 4 for details of these applications. In increasingly available high-dimensional settings where the dimension p diverges with, or is larger than, the number of independent or serially dependent observations n , the sample covariance matrix function $\widehat{\boldsymbol{\Sigma}}_y^S$ performs poorly and some regularization is needed. Fang et al. (2023) pioneered this effort by assuming approximate functional sparsity in $\boldsymbol{\Sigma}_y$, where the Hilbert–Schmidt norms of some $\Sigma_{y,jk}$'s are assumed zero or close to zero. Then they applied adaptive functional thresholding to the entries of $\widehat{\boldsymbol{\Sigma}}_y^S$ to achieve a consistent estimator of $\boldsymbol{\Sigma}_y$.

Such functional sparsity assumption, however, is restrictive or even unrealistic for many datasets, particularly in finance and economics, where variables often exhibit high correlations. E.g., in the stock market, the co-movement of intraday return curves (Horváth et al., 2014) is typically influenced by a small number of common market factors, leading to highly correlated functional variables. To alleviate the direct imposition of sparsity assumption, we employ the functional factor model (FFM) framework for $\mathbf{y}_t(\cdot)$, which decomposes it into two uncorrelated components, one common $\boldsymbol{\chi}_t(\cdot)$ driven by low-dimensional latent factors and one idiosyncratic $\boldsymbol{\varepsilon}_t(\cdot)$. We consider two types of FFM. The first type, explored in Guo et al. (2022), admits the representation with functional factors and scalar loadings:

$$\mathbf{y}_t(\cdot) = \boldsymbol{\chi}_t(\cdot) + \boldsymbol{\varepsilon}_t(\cdot) = \mathbf{B}\mathbf{f}_t(\cdot) + \boldsymbol{\varepsilon}_t(\cdot), \quad t = 1, \dots, n, \quad (1)$$

where $\mathbf{f}_t(\cdot)$ is a r -vector of stationary latent functional factors, \mathbf{B} is a $p \times r$ matrix of factor loadings and $\boldsymbol{\varepsilon}_t(\cdot)$ is a p -vector of idiosyncratic errors. The second type, introduced by Hallin et al. (2023), involves scalar factors and functional loadings:

$$\mathbf{y}_t(\cdot) = \boldsymbol{\chi}_t(\cdot) + \boldsymbol{\varepsilon}_t(\cdot) = \mathbf{Q}(\cdot)\boldsymbol{\gamma}_t + \boldsymbol{\varepsilon}_t(\cdot), \quad t = 1, \dots, n, \quad (2)$$

where $\boldsymbol{\gamma}_t$ is a r -vector of stationary latent factors and $\mathbf{Q}(\cdot)$ is a $p \times r$ matrix of functional factor loadings. We refer to $\boldsymbol{\Sigma}_f$, $\boldsymbol{\Sigma}_\chi$ and $\boldsymbol{\Sigma}_\varepsilon$ as the covariance matrix functions of \mathbf{f}_t , $\boldsymbol{\chi}_t$ and $\boldsymbol{\varepsilon}_t$, respectively.

Within the FFM framework, our goal is to estimate the covariance matrix function $\boldsymbol{\Sigma}_y = \boldsymbol{\Sigma}_\chi + \boldsymbol{\Sigma}_\varepsilon$. Inspired by Fan et al. (2013), we impose the approximately functional sparsity assumption on $\boldsymbol{\Sigma}_\varepsilon$ instead of $\boldsymbol{\Sigma}_y$ directly giving rise to the conditional functional sparsity structure in models (1) and (2). To effectively separate $\boldsymbol{\chi}_t(\cdot)$ from $\boldsymbol{\varepsilon}_t(\cdot)$, we rely on the spiked matrix model (Wang and Fan, 2017) and its functional generalization, i.e. a large nonnegative definite matrix or operator-valued matrix $\boldsymbol{\Lambda} = \mathbf{L} + \mathbf{S}$, where \mathbf{L} is low rank and its nonzero eigenvalues grow fast as p diverges, whereas all the eigenvalues of \mathbf{S} are bounded or grow much slower. The spikeness pattern ensures that the large signals are

concentrated on \mathbf{L} , which facilitates our estimation procedure. Specifically, for model (2), with the decomposition

$$\underbrace{\boldsymbol{\Sigma}_y(\cdot, *)}_{\mathbf{\Lambda}} = \underbrace{\mathbf{Q}(\cdot)\text{Cov}(\boldsymbol{\gamma}_t)\mathbf{Q}(\cdot)^{\text{T}}}_{\mathbf{L}} + \underbrace{\boldsymbol{\Sigma}_{\varepsilon}(\cdot, *)}_{\mathbf{S}}, \quad (3)$$

we perform MFPCA based on $\widehat{\boldsymbol{\Sigma}}_y^{\mathbf{S}}$, then estimate $\boldsymbol{\Sigma}_{\chi}$ using the leading r functional principal components and finally propose a novel adaptive functional thresholding procedure to estimate the sparse $\boldsymbol{\Sigma}_{\varepsilon}$. This results in a Functional Principal Orthogonal complement Thresholding (FPOET) estimator, extending the POET methodology for large covariance matrix estimation (Fan et al., 2013; 2018; Wang et al., 2021) to the functional domain. Alternatively, for model (1), considering the violation of nonnegative definiteness in $\boldsymbol{\Sigma}_y(u, v)$ for $u \neq v$, we utilize the nonnegative definite doubly integrated Gram covariance:

$$\underbrace{\int \int \boldsymbol{\Sigma}_y(u, v)\boldsymbol{\Sigma}_y(u, v)^{\text{T}}dudv}_{\mathbf{\Lambda}} = \underbrace{\mathbf{B}\left\{\int \int \boldsymbol{\Sigma}_f(u, v)\mathbf{B}^{\text{T}}\mathbf{B}\boldsymbol{\Sigma}_f(u, v)^{\text{T}}dudv\right\}\mathbf{B}^{\text{T}}}_{\mathbf{L}} + \underbrace{\text{remaining terms}}_{\mathbf{S}}, \quad (4)$$

which is shown to be identified asymptotically as $p \rightarrow \infty$. We propose to carry out eigenanalysis of the sample version of $\mathbf{\Lambda}$ in (4) combined with least squares to estimate \mathbf{B} , $\mathbf{f}_t(\cdot)$ and hence $\boldsymbol{\Sigma}_{\chi}$, and then employ the same thresholding method to estimate $\boldsymbol{\Sigma}_{\varepsilon}$. This yields an Eigenanalysis of Doubly Integrated Gram covariance and Thresholding (DIGIT) estimator.

The new contribution of this paper can be summarized in four key aspects. First, though our model (1) shares the same form as the one in Guo et al. (2022) and aligns with the direction of static factor models in Bai and Ng (2002) and Fan et al. (2013), substantial advances have been made in our methodology and theory: (i) We allow weak serial correlations in idiosyncratic components $\boldsymbol{\varepsilon}_t(\cdot)$ rather than assuming the white noise. (ii) Unlike the autocovariance-based method (Guo et al., 2022) for serially dependent data, we leverage the covariance information to propose a more efficient estimation procedure that encompasses independent observations as a special case. (iii) More importantly, under the pervasiveness assumption, we establish novel asymptotic identifiability in (4), where the first r eigenvalues of \mathbf{L} grow at rate $O(p^2)$, whereas all the eigenvalues of \mathbf{S} diverge at a rate slower than $O(p^2)$.

Second, for model (2), we extend the standard asymptotically identified covariance decomposition in Bai and Ng (2002) to the functional domain, under the functional counterpart of the pervasiveness assumption. Based on these findings, we provide mathematical insights when the functional factor analysis for models (1) and (2) and the proposed eigenanalysis of the respective $\mathbf{\Lambda}$'s in (3) and (4) are approximately the same for high-dimensional functional data/functional time series.

Third, we develop a new adaptive functional thresholding approach to estimate sparse Σ_ε . Compared to the competitor in Fang et al. (2023), our approach requires weaker assumptions while achieving similar finite-sample performance. Fourth, with the aid of such thresholding technique in conjunction with our estimation of FFMs (1) and (2), we propose two factor-guided covariance matrix function estimators, DIGIT and FPOET, respectively. We derive the associated convergence rates of estimators for Σ_ε , Σ_y and its inverse under various functional matrix norms. Additionally, we introduce fully functional information criteria to select the more suitable model between FFMs (1) and (2).

The rest of the paper is organized as follows. Section 2 presents the corresponding procedures for estimating Σ_y under two FFMs as well as the information criteria used for model selection. Section 3 provides the asymptotic theory for involved estimated quantities. Section 4 discusses a couple of applications of the proposed estimation. We assess the finite-sample performance of our proposal through extensive simulations in Section 5 and two real data applications in Section 6.

Throughout the paper, for any matrix $\mathbf{M} = (M_{ij})_{p \times q}$, we denote its matrices ℓ_1 norm, ℓ_∞ norm, operator norm, Frobenius norm and elementwise ℓ_∞ norm by $\|\mathbf{M}\|_1 = \max_j \sum_i |M_{ij}|$, $\|\mathbf{M}\|_\infty = \max_i \sum_j |M_{ij}|$, $\|\mathbf{M}\| = \lambda_{\max}^{1/2}(\mathbf{M}^T \mathbf{M})$, $\|\mathbf{M}\|_F = (\sum_{i,j} M_{ij}^2)^{1/2}$ and $\|\mathbf{M}\|_{\max} = \max_{i,j} |M_{ij}|$, respectively. Let $\mathbb{H} = L_2(\mathcal{U})$ be the Hilbert space of squared integrable functions defined on the compact set \mathcal{U} . We denote its p -fold Cartesian product by $\mathbb{H}^p = \mathbb{H} \times \cdots \times \mathbb{H}$ and tensor product by $\mathbb{S} = \mathbb{H} \otimes \mathbb{H}$. For $\mathbf{f} = (f_1, \dots, f_p)^T$, $\mathbf{g} = (g_1, \dots, g_p)^T \in \mathbb{H}^p$, we denote the inner product by $\langle \mathbf{f}, \mathbf{g} \rangle = \int_{\mathcal{U}} \mathbf{f}(u)^T \mathbf{g}(u) du$ with induced norm $\|\cdot\| = \langle \cdot, \cdot \rangle^{1/2}$. For an integral

matrix operator $\mathbf{K} : \mathbb{H}^p \rightarrow \mathbb{H}^q$ induced from the kernel matrix function $\mathbf{K} = \{K_{ij}(\cdot, \cdot)\}_{q \times p}$ with each $K_{ij} \in \mathbb{S}$, $\mathbf{K}(\mathbf{f})(\cdot) = \int_{\mathcal{U}} \mathbf{K}(\cdot, u) \mathbf{f}(u) du \in \mathbb{H}^q$ for any given $\mathbf{f} \in \mathbb{H}^p$. For notational economy, we will use \mathbf{K} to denote both the kernel function and the operator. We define the functional version of matrix ℓ_1 norm by $\|\mathbf{K}\|_{\mathcal{S},1} = \max_j \sum_i \|K_{ij}\|_{\mathcal{S}}$, where, for each $K_{ij} \in \mathbb{S}$, we denote its Hilbert–Schmidt norm by $\|K_{ij}\|_{\mathcal{S}} = \{\iint K_{ij}(u, v)^2 du dv\}^{1/2}$ and trace norm by $\|K_{ii}\|_{\mathcal{N}} = \int K_{ii}(u, u) du$ for $i = j$. Similarly, we define $\|\mathbf{K}\|_{\mathcal{S},\infty} = \max_i \sum_j \|K_{ij}\|_{\mathcal{S}}$, $\|\mathbf{K}\|_{\mathcal{S},\text{F}} = \{\sum_{i,j} \|K_{ij}\|_{\mathcal{S}}^2\}^{1/2}$ and $\|\mathbf{K}\|_{\mathcal{S},\text{max}} = \max_{i,j} \|K_{ij}\|_{\mathcal{S}}$ as the functional versions of matrix ℓ_∞ , Frobenius and elementwise ℓ_∞ norms, respectively. We define the operator norm by $\|\mathbf{K}\|_{\mathcal{L}} = \sup_{\mathbf{x} \in \mathbb{H}^p, \|\mathbf{x}\| \leq 1} \|\mathbf{K}(\mathbf{x})\|$. For a positive integer m , write $[m] = \{1, \dots, m\}$ and denote by \mathbf{I}_m the identity matrix of size $m \times m$. For $x, y \in \mathbb{R}$, we use $x \wedge y = \min(x, y)$. For two positive sequences $\{a_n\}$ and $\{b_n\}$, we write $a_n \lesssim b_n$ or $a_n = O(b_n)$ or $b_n \gtrsim a_n$ if there exists a positive constant c such that $a_n/b_n \leq c$, and $a_n = o(b_n)$ if $a_n/b_n \rightarrow 0$. We write $a_n \asymp b_n$ if and only if $a_n \lesssim b_n$ and $a_n \gtrsim b_n$ hold simultaneously.

2 Methodology

2.1 FFM with functional factors

Suppose that $\mathbf{y}_t(\cdot)$ admits FFM representation (1), where r common functional factors in $\mathbf{f}_t(\cdot) = \{f_{t1}(\cdot), \dots, f_{tr}(\cdot)\}^T$ are uncorrelated with the idiosyncratic errors $\boldsymbol{\varepsilon}_t(\cdot) = \{\varepsilon_{t1}(\cdot), \dots, \varepsilon_{tp}(\cdot)\}^T$ and r is assumed to be fixed. Then we have

$$\boldsymbol{\Sigma}_y(u, v) = \mathbf{B} \boldsymbol{\Sigma}_f(u, v) \mathbf{B}^T + \boldsymbol{\Sigma}_\varepsilon(u, v), \quad (u, v) \in \mathcal{U}^2, \quad (5)$$

which is not nonnegative definite for some u, v . To ensure nonnegative definiteness and accumulate covariance information as much as possible, we propose to perform an eigenanalysis of doubly integrated Gram covariance:

$$\boldsymbol{\Omega} = \int \int \boldsymbol{\Sigma}_y(u, v) \boldsymbol{\Sigma}_y(u, v)^T du dv \equiv \boldsymbol{\Omega}_{\mathcal{L}} + \boldsymbol{\Omega}_{\mathcal{R}}, \quad (6)$$

where $\boldsymbol{\Omega}_{\mathcal{L}} = \mathbf{B}\{\int\int \boldsymbol{\Sigma}_f(u, v)\mathbf{B}^\top\mathbf{B}\boldsymbol{\Sigma}_f(u, v)^\top dudv\}\mathbf{B}^\top$ and $\boldsymbol{\Omega}_{\mathcal{R}} = \int\int \boldsymbol{\Sigma}_\varepsilon(u, v)\boldsymbol{\Sigma}_\varepsilon(u, v)^\top dudv + \int\int \mathbf{B}\boldsymbol{\Sigma}_f(u, v)\mathbf{B}^\top\boldsymbol{\Sigma}_\varepsilon(u, v)^\top dudv + \int\int \boldsymbol{\Sigma}_\varepsilon(u, v)\mathbf{B}\boldsymbol{\Sigma}_f(u, v)^\top\mathbf{B}^\top dudv$. To make the decomposition (6) identifiable, we impose the following condition.

Assumption 1. $p^{-1}\mathbf{B}^\top\mathbf{B} = \mathbf{I}_r$ and $\int\int \boldsymbol{\Sigma}_f(u, v)\boldsymbol{\Sigma}_f(u, v)^\top dudv = \text{diag}(\theta_1, \dots, \theta_r)$, where there exist some constants $\bar{\theta} > \underline{\theta} > 0$ such that $\bar{\theta} > \theta_1 > \theta_2 > \dots > \theta_r > \underline{\theta}$.

Remark 1. Model (1) exhibits an identifiable issue as it remains unchanged if $\{\mathbf{B}, \mathbf{f}_t(\cdot)\}$ is replaced by $\{\mathbf{B}\mathbf{U}, \mathbf{U}^{-1}\mathbf{f}_t(\cdot)\}$ for any invertible matrix \mathbf{U} . Bai and Ng (2002) assumed two types of normalization for the scalar factor model: one is $p^{-1}\mathbf{B}^\top\mathbf{B} = \mathbf{I}_r$ and the other is $\text{Cov}(\mathbf{f}_t) = \mathbf{I}_p$. We adopt the first type for model (1) to simplify the calculation of the low rank matrix $\boldsymbol{\Omega}_{\mathcal{L}}$ in (6). However, this constraint alone is insufficient to identify \mathbf{B} , but the space spanned by the columns of $\mathbf{B} = (\mathbf{b}_1, \dots, \mathbf{b}_r)$. Hence, we introduce an additional constraint based on the diagonalization of $\int\int \boldsymbol{\Sigma}_f(u, v)\boldsymbol{\Sigma}_f(u, v)^\top dudv$, which is ensured by the fact that any nonnegative-definite matrix can be orthogonally diagonalized. Under Assumption 1, we can express $\boldsymbol{\Omega}_{\mathcal{L}} = \sum_{i=1}^r p\theta_i \mathbf{b}_i \mathbf{b}_i^\top$, implying that $\|\boldsymbol{\Omega}_{\mathcal{L}}\| \asymp \|\boldsymbol{\Omega}_{\mathcal{L}}\|_{\min} \asymp p^2$

We now elucidate why performing eigenanalysis of $\boldsymbol{\Omega}$ can be employed for functional factor analysis under model (1). Write $\tilde{\mathbf{B}} = p^{-1/2}\mathbf{B} = (\tilde{\mathbf{b}}_1, \dots, \tilde{\mathbf{b}}_r)$, which satisfies $\tilde{\mathbf{B}}^\top\tilde{\mathbf{B}} = \mathbf{I}_r$. Under Assumption 1, it holds that $\boldsymbol{\Omega}_{\mathcal{L}} = p^2 \sum_{i=1}^r \theta_i \tilde{\mathbf{b}}_i \tilde{\mathbf{b}}_i^\top$, whose eigenvalue/eigenvector pairs are $\{(p^2\theta_i, \tilde{\mathbf{b}}_i)\}_{i \in [r]}$. Let $\lambda_1 \geq \dots \geq \lambda_p$ be the ordered eigenvalues of $\boldsymbol{\Omega}$ and $\boldsymbol{\xi}_1, \dots, \boldsymbol{\xi}_p$ be the corresponding eigenvectors. We then have the following proposition.

Proposition 1. Suppose that Assumption 1 and $\|\boldsymbol{\Omega}_{\mathcal{R}}\| = o(p^2)$ hold. Then we have

- (i) $|\lambda_j - p^2\theta_j| \leq \|\boldsymbol{\Omega}_{\mathcal{R}}\|$ for $j \in [r]$ and $|\lambda_j| \leq \|\boldsymbol{\Omega}_{\mathcal{R}}\|$ for $j \in [p] \setminus [r]$;
- (ii) $\|\boldsymbol{\xi}_j - \tilde{\mathbf{b}}_j\| = O(p^{-2}\|\boldsymbol{\Omega}_{\mathcal{R}}\|)$ for $j \in [r]$.

Proposition 1 indicates that we can distinguish the leading eigenvalues $\{\lambda_j\}_{j \in [r]}$ from the remaining eigenvalues, and ensure the approximate equivalence between eigenvectors $\{\boldsymbol{\xi}_j\}_{j \in [r]}$ and the normalized factor loading columns $\{\tilde{\mathbf{b}}_j\}_{j \in [r]}$, provided that $\|\boldsymbol{\Omega}_{\mathcal{R}}\| = o(p^2)$. Towards

this, we impose an approximately functional sparsity condition on Σ_ε measured through

$$s_p = \max_{i \in [p]} \sum_{j=1}^p \|\sigma_i\|_{\mathcal{N}}^{(1-q)/2} \|\sigma_j\|_{\mathcal{N}}^{(1-q)/2} \|\Sigma_{\varepsilon,ij}\|_{\mathcal{S}}^q, \quad \text{for some } q \in [0, 1), \quad (7)$$

where $\sigma_i(u) = \Sigma_{\varepsilon,ii}(u, u)$ for $u \in \mathcal{U}$ and $i \in [p]$. Specially, when $q = 0$ and $\{\|\sigma_i\|_{\mathcal{N}}\}$ are bounded, s_p can be simplified to the exact functional sparsity, i.e., $\max_i \sum_j I(\|\Sigma_{\varepsilon,ij}\|_{\mathcal{S}} \neq 0)$.

Remark 2. *Our proposed measure of functional sparsity in (7) for non-functional data degenerates to the measure of sparsity adopted in Cai and Liu (2011). It is worth mentioning that Fang et al. (2023) introduced a different measure of functional sparsity as*

$$\tilde{s}_p = \max_{i \in [p]} \sum_{j=1}^p \|\sigma_i\|_{\infty}^{(1-q)/2} \|\sigma_j\|_{\infty}^{(1-q)/2} \|\Sigma_{\varepsilon,ij}\|_{\mathcal{S}}^q,$$

where $\|\sigma_i\|_{\infty} = \sup_{u \in \mathcal{U}} \sigma_i(u) \geq \|\sigma_i\|_{\mathcal{N}}$. As a result, we will use s_p instead of \tilde{s}_p .

(ii) With bounded $\{\|\sigma_i\|_{\mathcal{N}}\}$, we can easily obtain $\|\Sigma_\varepsilon\|_{\mathcal{S},1} = \|\Sigma_\varepsilon\|_{\mathcal{S},\infty} = O(s_p)$, which, along with Lemmas A6, B10 of the Supplementary Material and Assumption 1, yields that

$$\|\Omega_{\mathcal{R}}\| \leq \|\Sigma_\varepsilon\|_{\mathcal{S},\infty} \|\Sigma_\varepsilon\|_{\mathcal{S},1} + 2(\|\mathbf{B}\Sigma_f\mathbf{B}^T\|_{\mathcal{S},\infty} \|\mathbf{B}\Sigma_f\mathbf{B}^T\|_{\mathcal{S},1})^{1/2} (\|\Sigma_\varepsilon\|_{\mathcal{S},1} \|\Sigma_\varepsilon\|_{\mathcal{S},\infty})^{1/2} = O(s_p^2 + ps_p).$$

Hence, when $s_p = o(p)$, Proposition 1 implies that functional factor analysis under model (1) and eigenanalysis of Ω are approximately the same for high-dimensional functional data.

To estimate model (1), we assume the number of functional factors (i.e., r) is known, and will introduce a data-driven approach to determine it in Section 2.3. Without loss of generality, we assume that $\mathbf{y}_t(\cdot)$ has been centered to have mean zero. The sample covariance matrix function of $\Sigma_y(\cdot, \cdot)$ is given by $\hat{\Sigma}_y^s(u, v) = n^{-1} \sum_{t=1}^n \mathbf{y}_t(u) \mathbf{y}_t(v)^T$. Performing eigen-decomposition on the sample version of Ω ,

$$\hat{\Omega} = \int \int \hat{\Sigma}_y^s(u, v) \hat{\Sigma}_y^s(u, v)^T du dv, \quad (8)$$

leads to estimated eigenvalues $\hat{\lambda}_1, \dots, \hat{\lambda}_p$ and their associated eigenvectors $\hat{\boldsymbol{\xi}}_1, \dots, \hat{\boldsymbol{\xi}}_p$. Then the estimated factor loading matrix is $\hat{\mathbf{B}} = \sqrt{p}(\hat{\boldsymbol{\xi}}_1, \dots, \hat{\boldsymbol{\xi}}_r) = (\hat{\mathbf{b}}_1, \dots, \hat{\mathbf{b}}_r)$.

To estimate functional factors $\{\mathbf{f}_t(\cdot)\}_{t \in [n]}$, we minimize the least squares criterion

$$\sum_{t=1}^n \|\mathbf{y}_t - \widehat{\mathbf{B}}\mathbf{f}_t\|^2 = \sum_{t=1}^n \int_{\mathcal{U}} \{\mathbf{y}_t(u) - \widehat{\mathbf{B}}\mathbf{f}_t(u)\}^T \{\mathbf{y}_t(u) - \widehat{\mathbf{B}}\mathbf{f}_t(u)\} du \quad (9)$$

with respect to $\mathbf{f}_1(\cdot), \dots, \mathbf{f}_n(\cdot)$. By setting the functional derivatives to zero, we obtain the least squares estimator $\widehat{\mathbf{f}}_t(\cdot) = p^{-1}\widehat{\mathbf{B}}^T\mathbf{y}_t(\cdot)$ and the estimated idiosyncratic errors are given by $\widehat{\boldsymbol{\varepsilon}}_t(\cdot) = (\mathbf{I}_p - p^{-1}\widehat{\mathbf{B}}\widehat{\mathbf{B}}^T)\mathbf{y}_t(\cdot)$. Hence, we can obtain sample covariance matrix functions of estimated common factors and estimated idiosyncratic errors as $\widehat{\boldsymbol{\Sigma}}_f(u, v) = n^{-1} \sum_{t=1}^n \widehat{\mathbf{f}}_t(u)\widehat{\mathbf{f}}_t(v)^T$ and $\widehat{\boldsymbol{\Sigma}}_\varepsilon(u, v) = \{\widehat{\boldsymbol{\Sigma}}_{\varepsilon, ij}(u, v)\}_{p \times p} = \sum_{t=1}^n n^{-1} \widehat{\boldsymbol{\varepsilon}}_t(u)\widehat{\boldsymbol{\varepsilon}}_t(v)^T$, respectively.

Since $\boldsymbol{\Sigma}_\varepsilon$ is assumed to be functional sparse, we introduce an adaptive functional thresholding (AFT) estimator of $\boldsymbol{\Sigma}_\varepsilon$. To this end, we define the functional variance factors $\Theta_{ij}(u, v) = \text{Var}\{\varepsilon_{ti}(u)\varepsilon_{tj}(v)\}$ for $i, j \in [p]$, whose estimators are

$$\widehat{\Theta}_{ij}(u, v) = \frac{1}{n} \sum_{t=1}^n \{\widehat{\varepsilon}_{ti}(u)\widehat{\varepsilon}_{tj}(v) - \widehat{\boldsymbol{\Sigma}}_{\varepsilon, ij}(u, v)\}^2,$$

with $\widehat{\varepsilon}_{ti}(\cdot) = y_{ti}(\cdot) - \check{\mathbf{b}}_i^T \widehat{\mathbf{f}}_t(\cdot)$ and $\check{\mathbf{b}}_i$ being the i -th row vector of $\widehat{\mathbf{B}}$. We develop an AFT procedure on $\widehat{\boldsymbol{\Sigma}}_\varepsilon$ using entry-dependent functional thresholds that automatically adapt to the variability of $\widehat{\boldsymbol{\Sigma}}_{\varepsilon, ij}$'s. Specifically, the AFT estimator is defined as $\widehat{\boldsymbol{\Sigma}}_\varepsilon^A = \{\widehat{\boldsymbol{\Sigma}}_{\varepsilon, ij}^A(\cdot, \cdot)\}_{p \times p}$

$$\widehat{\boldsymbol{\Sigma}}_{\varepsilon, ij}^A = \|\widehat{\Theta}_{ij}^{1/2}\|_{\mathcal{S}} \times s_\lambda\left(\widehat{\boldsymbol{\Sigma}}_{\varepsilon, ij} / \|\widehat{\Theta}_{ij}^{1/2}\|_{\mathcal{S}}\right) \text{ with } \lambda = \dot{C} \left(\sqrt{\frac{\log p}{n}} + \frac{1}{\sqrt{p}} \right), \quad (10)$$

where $\dot{C} > 0$ is a pre-specified constant that can be selected via multifold cross-validation and the order $\sqrt{\log p/n} + 1/\sqrt{p}$ is related to the convergence rate of $\widehat{\boldsymbol{\Sigma}}_{\varepsilon, ij} / \|\widehat{\Theta}_{ij}^{1/2}\|_{\mathcal{S}}$ under functional elementwise ℓ_∞ norm. Here s_λ is a functional thresholding operator with regularization parameter $\lambda \geq 0$ (Fang et al., 2023) and belongs to the class $s_\lambda : \mathbb{S} \rightarrow \mathbb{S}$ satisfying: (i) $\|s_\lambda(Z)\|_{\mathcal{S}} \leq c\|Y\|_{\mathcal{S}}$ for all $Z, Y \in \mathbb{S}$ that satisfy $\|Z - Y\|_{\mathcal{S}} \leq \lambda$ and some $c > 0$; (ii) $\|s_\lambda(Z)\|_{\mathcal{S}} = 0$ for $\|Z\|_{\mathcal{S}} \leq \lambda$; (iii) $\|s_\lambda(Z) - Z\|_{\mathcal{S}} \leq \lambda$ for all $Z \in \mathbb{S}$. This class includes functional versions of commonly adopted thresholding functions, such as hard thresholding, soft thresholding, smoothed clipped absolute deviation (Fan and Li, 2001), and the adaptive lasso (Zou, 2006).

Remark 3. By comparison, Fang et al. (2023) introduced an alternative AFT estimator

$$\widetilde{\boldsymbol{\Sigma}}_\varepsilon^A = (\widetilde{\boldsymbol{\Sigma}}_{\varepsilon, ij}^A)_{p \times p} \text{ with } \widetilde{\boldsymbol{\Sigma}}_{\varepsilon, ij}^A = \widehat{\Theta}_{ij}^{1/2} \times s_\lambda\left(\widehat{\boldsymbol{\Sigma}}_{\varepsilon, ij} / \widehat{\Theta}_{ij}^{1/2}\right), \quad (11)$$

which uses a single threshold level to functionally threshold standardized entries $\widehat{\Sigma}_{\varepsilon,ij}/\widehat{\Theta}_{ij}^{1/2}$ across all (i,j) , resulting in entry-dependent functional thresholds for $\widehat{\Sigma}_{\varepsilon,ij}$. Since $\widetilde{\Sigma}_{\varepsilon,jk}^A$ requires stronger assumptions (see Remark 2 above and the remark for Assumption 5 below), we adopt the AFT estimator $\widehat{\Sigma}_{\varepsilon,jk}^A$ leading to comparable empirical performance (see Section F of the Supplementary Material).

Finally, we obtain an Eigenanalysis of Doubly Integrated Gram covariance and Thresholding (DIGIT) estimator of Σ_y as

$$\widehat{\Sigma}_y^D(u, v) = \widehat{\mathbf{B}}\widehat{\Sigma}_f(u, v)\widehat{\mathbf{B}}^T + \widehat{\Sigma}_\varepsilon^A(u, v), \quad (u, v) \in \mathcal{U}^2. \quad (12)$$

2.2 FFM with functional loadings

The structure of FFM is not unique. We could also assume $\mathbf{y}_t(\cdot)$ satisfies FFM (2) with scalar factors and functional loadings $\mathbf{Q}(\cdot) = \{\mathbf{q}_1(\cdot), \dots, \mathbf{q}_p(\cdot)\}^T$ with each $\mathbf{q}_i(\cdot) \in \mathbb{H}^r$, where r common scalar factors $\boldsymbol{\gamma}_t = (\gamma_{t1}, \dots, \gamma_{tr})^T$ are uncorrelated with the idiosyncratic errors in $\boldsymbol{\varepsilon}_t(\cdot)$ and r is assumed to be fixed. Then we have the covariance decomposition

$$\Sigma_y(u, v) = \mathbf{Q}(u)\Sigma_\gamma\mathbf{Q}(v)^T + \Sigma_\varepsilon(u, v), \quad (u, v) \in \mathcal{U}^2. \quad (13)$$

By Mercer's theorem (Carmeli et al., 2006), which serves as the foundation of MFPCA (Happ and Greven, 2018), there exists an orthonormal basis consisting of eigenfunctions $\{\boldsymbol{\varphi}_i(\cdot)\}_{i=1}^\infty$ of Σ_y and the associated eigenvalues $\tau_1 \geq \tau_2 \geq \dots \geq 0$ such that

$$\Sigma_y(u, v) = \sum_{i=1}^{\infty} \tau_i \boldsymbol{\varphi}_i(u) \boldsymbol{\varphi}_i(v)^T, \quad (u, v) \in \mathcal{U}^2. \quad (14)$$

We now provide mathematical insights into why MFPCA can be applied for functional factor analysis under model (2). To ensure the identifiability of the decomposition in (13), we impose a normalization-type condition similar to Assumption 1.

Assumption 1'. $\Sigma_\gamma = \mathbf{I}_r$ and $p^{-1} \int \mathbf{Q}(u)^T \mathbf{Q}(u) du = \text{diag}(\vartheta_1, \dots, \vartheta_r)$, where there exist some constants $\bar{\vartheta} > \underline{\vartheta} > 0$ such that $\bar{\vartheta} > \vartheta_1 > \vartheta_2 > \dots > \vartheta_r > \underline{\vartheta}$.

Suppose Assumption 1' holds, and let $\tilde{\mathbf{q}}_1(\cdot), \dots, \tilde{\mathbf{q}}_r(\cdot)$ be the normalized columns of $\mathbf{Q}(\cdot)$ such that $\|\tilde{\mathbf{q}}_j\| = 1$ for $j \in [r]$. By Lemma A9 of the Supplementary Material, $\{\tilde{\mathbf{q}}_j(\cdot)\}_{j \in [r]}$ are the orthonormal eigenfunctions of the kernel function $\mathbf{Q}(\cdot)\mathbf{Q}(\cdot)^\top$ with corresponding eigenvalues $\{p\vartheta_j\}_{j=1}^r$ and the rest 0. We then give the following proposition.

Proposition 2. *Suppose that Assumption 1' and $\|\boldsymbol{\Sigma}_\varepsilon\|_{\mathcal{L}} = o(p)$ hold. Then we have*

- (i) $|\tau_j - p\vartheta_j| \leq \|\boldsymbol{\Sigma}_\varepsilon\|_{\mathcal{L}}$ for $j \in [r]$ and $|\tau_j| \leq \|\boldsymbol{\Sigma}_\varepsilon\|_{\mathcal{L}}$ for $j \in [p] \setminus [r]$;
- (ii) $\|\boldsymbol{\varphi}_j - \tilde{\mathbf{q}}_j\| = O(p^{-1}\|\boldsymbol{\Sigma}_\varepsilon\|_{\mathcal{L}})$ for $j \in [r]$.

Proposition 2 implies that, if we can prove $\|\boldsymbol{\Sigma}_\varepsilon\|_{\mathcal{L}} = o(p)$, then we can distinguish the principle eigenvalues $\{\tau_j\}_{j \in [r]}$ from the remaining eigenvalues. Additionally, the first r eigenfunctions $\{\boldsymbol{\varphi}_j(\cdot)\}_{j \in [r]}$ are approximately the same as the normalized columns of $\{\tilde{\mathbf{q}}_j(\cdot)\}_{j \in [r]}$. To establish this, we impose the same functional sparsity condition on $\boldsymbol{\Sigma}_\varepsilon$ as measured by s_p in (7). Applying Lemma A7(iii) of the Supplementary Material, we have $\|\boldsymbol{\Sigma}_\varepsilon\|_{\mathcal{L}} \leq \|\boldsymbol{\Sigma}_\varepsilon\|_{\mathcal{S},1}^{1/2}\|\boldsymbol{\Sigma}_\varepsilon\|_{\mathcal{S},\infty}^{1/2} = O(s_p)$. Hence, when $s_p = o(p)$, MFPCA is approximately equivalent to functional factor analysis under model (2) for high-dimensional functional data.

We now present the estimation procedure assuming that r is known, and we will develop a ratio-based approach to identify r in Section 2.3. Let $\hat{\tau}_1 \geq \hat{\tau}_2 \cdots \geq 0$ be the eigenvalues of the sample covariance $\hat{\boldsymbol{\Sigma}}_y^S$ and $\{\hat{\boldsymbol{\varphi}}_j(\cdot)\}_{j=1}^\infty$ be their corresponding eigenfunctions. Then $\hat{\boldsymbol{\Sigma}}_y^S$ has the spectral decomposition

$$\hat{\boldsymbol{\Sigma}}_y^S(u, v) = \sum_{j=1}^r \hat{\tau}_j \hat{\boldsymbol{\varphi}}_j(u) \hat{\boldsymbol{\varphi}}_j(v)^\top + \hat{\mathbf{R}}(u, v),$$

where $\hat{\mathbf{R}}(u, v) = \sum_{j=r+1}^\infty \hat{\tau}_j \hat{\boldsymbol{\varphi}}_j(u) \hat{\boldsymbol{\varphi}}_j(v)^\top$ is the functional principal orthogonal complement.

Applying AFT as introduced in Section 2.1 to $\hat{\mathbf{R}}$ yields the estimator $\hat{\mathbf{R}}^A$. Finally, we obtain a Functional Principal Orthogonal complement Thresholding (FPOET) estimator as

$$\hat{\boldsymbol{\Sigma}}_y^{\mathcal{F}}(u, v) = \sum_{j=1}^r \hat{\tau}_j \hat{\boldsymbol{\varphi}}_j(u) \hat{\boldsymbol{\varphi}}_j(v)^\top + \hat{\mathbf{R}}^A(u, v). \quad (15)$$

It is noteworthy that, with $\boldsymbol{\Sigma}_y$ satisfying decompositions (5) and (13) under FFMs (1) and (2), respectively, both DIGIT and FPOET methods embrace the fundamental concept of

a “low-rank plus sparse” representation generalized to the functional setting. Consequently, the common estimation steps involve applying PCA or MFPCA to estimate the factor loadings, and applying AFT to estimate sparse Σ_ε . Essentially, these two methods are closely related, allowing the proposed estimators to exhibit empirical robustness even in cases of model misspecification (See details in Section 5). See also Section E.2 of the Supplementary Material for a discussion about the relationship between two FFM.

We next present an equivalent representation of FPOET estimator (15) from a least squares perspective. We consider solving a constraint least squares minimization problem:

$$\{\widehat{\mathbf{Q}}(\cdot), \widehat{\mathbf{\Gamma}}\} = \arg \min_{\mathbf{Q}(\cdot), \mathbf{\Gamma}} \int \|\mathbf{Y}(u) - \mathbf{Q}(u)\mathbf{\Gamma}^\top\|_{\mathbb{F}}^2 du = \arg \min_{\mathbf{Q}(\cdot), \gamma_1, \dots, \gamma_n} \sum_{t=1}^n \|\mathbf{y}_t - \mathbf{Q}\gamma_t\|^2, \quad (16)$$

subject to the normalization constraint corresponding to Assumption 1', i.e.,

$$\frac{1}{n} \sum_{t=1}^n \gamma_t \gamma_t^\top = \mathbf{I}_r \quad \text{and} \quad \frac{1}{p} \int \mathbf{Q}(u)^\top \mathbf{Q}(u) du \text{ is diagonal,}$$

where $\mathbf{Y}(\cdot) = \{\mathbf{y}_1(\cdot), \dots, \mathbf{y}_n(\cdot)\}$ and $\mathbf{\Gamma}^\top = (\gamma_1, \dots, \gamma_n)$. Given each $\mathbf{\Gamma}$, setting the functional derivative of the objective in (16) w.r.t. $\mathbf{Q}(\cdot)$ to zero, we obtain the constrained least squares estimator $\widetilde{\mathbf{Q}}(\cdot) = n^{-1}\mathbf{Y}(\cdot)\mathbf{\Gamma}$. Plugging it into (16), the objective as a function of $\mathbf{\Gamma}$ becomes $\int \|\mathbf{Y}(u) - n^{-1}\mathbf{Y}(u)\mathbf{\Gamma}\mathbf{\Gamma}^\top\|_{\mathbb{F}}^2 du = \int \text{tr}\{(\mathbf{I}_n - n^{-1}\mathbf{\Gamma}\mathbf{\Gamma}^\top)\mathbf{Y}(u)^\top \mathbf{Y}(u)\} du$, the minimizer of which is equivalent to the maximizer of $\text{tr}[\mathbf{\Gamma}^\top \{ \int \mathbf{Y}(u)^\top \mathbf{Y}(u) du \} \mathbf{\Gamma}]$. This implies that the columns of $n^{-1/2}\widehat{\mathbf{\Gamma}}$ are the eigenvectors corresponding to the r largest eigenvalues of $\int \mathbf{Y}(u)^\top \mathbf{Y}(u) du \in \mathbb{R}^{n \times n}$, and then $\widehat{\mathbf{Q}}(\cdot) = n^{-1}\mathbf{Y}(\cdot)\widehat{\mathbf{\Gamma}}$.

Let $\widetilde{\boldsymbol{\varepsilon}}_t(\cdot) = \mathbf{y}_t(\cdot) - \widehat{\mathbf{Q}}(\cdot)\widehat{\boldsymbol{\gamma}}_t$ and $\widetilde{\boldsymbol{\Sigma}}_\varepsilon(u, v) = n^{-1} \sum_{t=1}^n \widetilde{\boldsymbol{\varepsilon}}_t(u)\widetilde{\boldsymbol{\varepsilon}}_t(v)^\top$. Applying our proposed AFT in (10) to $\widetilde{\boldsymbol{\Sigma}}_\varepsilon$ yields the estimator $\widetilde{\boldsymbol{\Sigma}}_\varepsilon^{\mathcal{A}}$. Analogous to the decomposition (13) under Assumption 1', we propose the following substitution estimator

$$\widehat{\boldsymbol{\Sigma}}_y^{\mathcal{L}}(u, v) = \widehat{\mathbf{Q}}(u)\widehat{\mathbf{Q}}(v)^\top + \widetilde{\boldsymbol{\Sigma}}_\varepsilon^{\mathcal{A}}(u, v). \quad (17)$$

The following proposition reveals the equivalence between the FPOET estimator (15) and the constrained least squares estimator (17).

Proposition 3. *Suppose the same regularization parameters are used when applying AFT to $\hat{\mathbf{R}}$ and $\tilde{\Sigma}_\varepsilon$. Then we have $\hat{\Sigma}_y^{\mathcal{F}} = \hat{\Sigma}_y^{\mathcal{L}}$ and $\hat{\mathbf{R}}^{\mathcal{A}} = \tilde{\Sigma}_\varepsilon^{\mathcal{A}}$.*

Remark 4. (i) *While our FFM (2) shares the same form as the model studied in Tavakoli et al. (2023), which focused on the estimation of scalar factors and functional loadings from a least squares viewpoint, the main purpose of this paper lies in the estimation of large covariance matrix function. Consequently, we also propose a least-squares-based estimator of Σ_y , which turns out to be equivalent to our FPOET estimator by Proposition 3.*

(ii) *Using a similar procedure, we can also develop an alternative estimator for Σ_y under FFM (1) from a least squares perspective. However, this estimator is distinct from the DIGIT estimator (12) and leads to declined estimation efficiency. See detailed discussion in Section E.1 of the Supplementary Material.*

2.3 Determining the number of factors

We have developed the estimation procedures for FFMs (1) and (2), assuming the known number of functional or scalar factors (i.e. r). In this section, we take the frequently-used ratio-based approach (Lam and Yao, 2012; Wang et al., 2021) to determine the value of r .

Under model (1), we let $\hat{\lambda}_1 \geq \dots \geq \hat{\lambda}_p$ be the ordered eigenvalues of $\hat{\Omega}$ in (8), and propose to estimate r by

$$\hat{r}^{\mathcal{D}} = \arg \min_{r \in [c_r p]} \hat{\lambda}_{r+1} / \hat{\lambda}_r, \quad (18)$$

where we typically take $c_r = 0.75$ to circumvent the fluctuations caused by extremely small values. In practical implementation, we set $\hat{\lambda}_i/p^2$ to be 0 if its value is smaller than a pre-specified small threshold ε_0 (e.g., 0.01), and treat the ratio $0/0$ as 1. Hence, $\hat{\lambda}_{i+1}/\hat{\lambda}_i = (\hat{\lambda}_{i+1}/p^2)/(\hat{\lambda}_i/p^2) = 0/0 = 1$ if neither $\hat{\lambda}_{i+1}/p^2$ nor $\hat{\lambda}_i/p^2$ exceeds ε_0 as $p \rightarrow \infty$.

For model (2), we employ a similar eigenvalue-ratio estimator given by:

$$\hat{r}^{\mathcal{F}} = \arg \min_{r \in [r_0]} \hat{\tau}_{r+1} / \hat{\tau}_r, \quad (19)$$

where $\{\hat{\tau}_i\}_{i=1}^\infty$ represents the ordered eigenvalues of the sample covariance $\widehat{\boldsymbol{\Sigma}}_y^S(\cdot, \cdot)$. Similar to the previous case, we set $\hat{\tau}_i/p$ as 0 if its value is smaller than ϵ_0 and $0/0 = 1$.

2.4 Model selection criterion

A natural question that arises is which of the two candidate FFMs (1) and (2) is more appropriate for modeling $\{\mathbf{y}_t(\cdot)\}$. This section develops fully functional information criteria based on observed data for model selection.

When r functional factors are estimated under FFM (1), motivated from the least squares criterion (9), we define the mean squared residuals as

$$V^{\mathcal{D}}(r) = (pn)^{-1} \sum_{t=1}^n \|\mathbf{y}_t - p^{-1} \widehat{\mathbf{B}}_r \widehat{\mathbf{B}}_r^T \mathbf{y}_t\|^2,$$

where $\widehat{\mathbf{B}}_r$ is the estimated factor loading matrix by DIGIT. Analogously, when r scalar factors are estimated under FFM (2), it follows from the objective function in (16) that the corresponding mean squared residuals is

$$V^{\mathcal{F}}(r) = (pn)^{-1} \sum_{t=1}^n \|\mathbf{y}_t - n^{-1} \mathbf{Y} \widehat{\boldsymbol{\Gamma}}_r \widehat{\boldsymbol{\gamma}}_{t,r}\|^2,$$

where $\widehat{\boldsymbol{\Gamma}}_r^T = (\widehat{\boldsymbol{\gamma}}_{1,r}, \dots, \widehat{\boldsymbol{\gamma}}_{n,r})$ is formed by estimated factors using FPOET.

For any given r , we propose the following information criteria:

$$\begin{aligned} \text{PC}^{\mathcal{D}}(r) &= V^{\mathcal{D}}(r) + rg(p, n), & \text{IC}^{\mathcal{D}}(r) &= \log V^{\mathcal{D}}(r) + rg(p, n), \\ \text{PC}^{\mathcal{F}}(r) &= V^{\mathcal{F}}(r) + rg(p, n), & \text{IC}^{\mathcal{F}}(r) &= \log V^{\mathcal{F}}(r) + rg(p, n), \end{aligned} \tag{20}$$

where $g(p, n)$ is a penalty function of (p, n) . While there is much existing literature (c.f. Bai and Ng, 2002; Fan et al., 2013) that has adopted this type of criterion for identifying the number of factors in scalar factor models, we propose fully functional criteria for selecting the more appropriate FFM. Following Bai and Ng (2002), we suggest three examples of penalty functions, referred to as PC_1 , PC_2 , PC_3 and IC_1 , IC_2 , IC_3 , respectively, in the penalized loss functions (20),

$$(i) \ g(p, n) = \frac{p+n}{pn} \log \left(\frac{pn}{p+n} \right), \quad (ii) \ g(p, n) = \frac{p+n}{pn} \log(p \wedge n), \quad (iii) \ g(p, n) = \frac{\log(p \wedge n)}{p \wedge n}.$$

For model selection, we define the differences in the corresponding information criteria between the two FFM's as $\Delta\text{PC}_i = \text{PC}_i^{\mathcal{D}}(\hat{r}^{\mathcal{D}}) - \text{PC}_i^{\mathcal{F}}(\hat{r}^{\mathcal{F}})$ and $\Delta\text{IC}_i = \text{IC}_i^{\mathcal{D}}(\hat{r}^{\mathcal{D}}) - \text{IC}_i^{\mathcal{F}}(\hat{r}^{\mathcal{F}})$ for $i = 1, 2, 3$. The negative (or positive) values of ΔPC_i 's and ΔIC_i 's indicate that FFM (1) (or FFM (2)) is more suitable based on the observed data $\{\mathbf{y}_t(\cdot)\}_{t \in [n]}$.

3 Theory

3.1 Assumptions

The assumptions for models (1) and (2) exhibit a close one-to-one correspondence. For clarity, we will present them separately in a pairwise fashion.

Assumption 2. For model (1), $\{\mathbf{f}_t(\cdot)\}_{t \geq 1}$ and $\{\boldsymbol{\varepsilon}_t(\cdot)\}_{t \geq 1}$ are weakly stationary and $\mathbb{E}\{\varepsilon_{ti}(u)\} = \mathbb{E}\{\varepsilon_{ti}(u)f_{tj}(v)\} = 0$ for all $i \in [p], j \in [r]$ and $(u, v) \in \mathcal{U}^2$.

Assumption 2'. For model (2), $\{\boldsymbol{\gamma}_t\}_{t \geq 1}$ and $\{\boldsymbol{\varepsilon}_t(\cdot)\}_{t \geq 1}$ are weakly stationary and $\mathbb{E}\{\varepsilon_{ti}(u)\} = \mathbb{E}\{\varepsilon_{ti}(u)\boldsymbol{\gamma}_{tj}\} = 0$ for all $i \in [p], j \in [r]$ and $u \in \mathcal{U}$.

Assumption 3. For model (1), there exists some constant $C > 0$ such that, for all $j \in [r]$, $t \in [n]$, (i) $\|\mathbf{b}_j\|_{\max} < C$, (ii) $\mathbb{E}\|p^{-1/2}\boldsymbol{\varepsilon}_t\|^4 < C$, (iii) $\|\boldsymbol{\Sigma}_\varepsilon\|_{\mathcal{L}} < C$, (iv) $\max_{i \in [p]} \|\Sigma_{\varepsilon, ii}\|_{\mathcal{N}} < C$.

Assumption 3'. For model (2), there exists some constant $C' > 0$ such that, for all $i \in [p]$, $t, t' \in [n]$: (i) $\|\mathbf{q}_i\| < C'$, (ii) $\mathbb{E}\|p^{-1/2} \sum_{i=1}^p \int \mathbf{q}_i(u)\varepsilon_{ti}(u)du\|^4 < C'$ and $\mathbb{E}\{p^{-1/2}[\langle \boldsymbol{\varepsilon}_t, \boldsymbol{\varepsilon}_{t'} \rangle - \mathbb{E}\langle \boldsymbol{\varepsilon}_t, \boldsymbol{\varepsilon}_{t'} \rangle]\}^4 < C'$, (iii) $\|\boldsymbol{\Sigma}_\varepsilon\|_{\mathcal{L}} < C'$, (iv) $\max_{i \in [p]} \|\Sigma_{\varepsilon, ii}\|_{\mathcal{N}} < C'$.

Assumption 3(i) or 3'(i) requires the functional or scalar factors to be pervasive in the sense they influence a large fraction of the functional outcomes. Such pervasiveness-type assumption is commonly imposed in the literature (Bai, 2003; Fan et al., 2013). Assumption 3(ii) involves a standard moment constraint. Assumption 3'(ii) is needed to estimate scalar factors and functional loadings consistently. Assumption 3(iii) and 3'(iii) generalize the standard conditions for scalar factor models (Fan et al., 2018; Wang et al., 2021) to the

functional domain. Assumptions 3(iv) and 3'(iv) are for technical convenience. However we can relax them by allowing $\max_i \|\Sigma_{\varepsilon, ii}\|_{\mathcal{N}}$ to grow at some slow rate as p increases.

We use the functional stability measure (Guo and Qiao, 2023) to characterize the serial dependence. For $\{\mathbf{y}_t(\cdot)\}$, denote its autocovariance matrix functions by $\Sigma_y^{(h)}(u, v) = \text{Cov}\{\mathbf{y}_t(u), \mathbf{y}_{t+h}(v)\}$ for $h \in \mathbb{Z}$ and $(u, v) \in \mathcal{U}^2$ and its spectral density matrix function at frequency $\theta \in [-\pi, \pi]$ by $\mathbf{f}_{y, \theta}(u, v) = (2\pi)^{-1} \sum_{h \in \mathbb{Z}} \Sigma_y^{(h)}(u, v) \exp(-ih\theta)$. The functional stability measure of $\{\mathbf{y}_t(\cdot)\}$ is defined as

$$\mathcal{M}_y = 2\pi \cdot \operatorname{ess\,sup}_{\theta \in [-\pi, \pi], \phi \in \mathbb{H}_0^p} \frac{\langle \phi, \mathbf{f}_{y, \theta}(\phi) \rangle}{\langle \phi, \Sigma_y(\phi) \rangle},$$

where $\Sigma_y(\phi)(\cdot) = \int_{\mathcal{U}} \Sigma_y(\cdot, v) \phi(v) dv$ and $\mathbb{H}_0^p = \{\phi \in \mathbb{H}^p : \langle \phi, \Sigma_y(\phi) \rangle \in (0, \infty)\}$. When $\mathbf{y}_1(\cdot), \dots, \mathbf{y}_n(\cdot)$ are independent, $\mathcal{M}_y = 1$. See also Guo and Qiao (2023) for examples satisfying $\mathcal{M}_y < \infty$, such as functional moving average model and functional linear process. Similarly, we can define \mathcal{M}_ε of $\{\varepsilon_t(\cdot)\}$. To derive relevant exponential-type tails used in convergence analysis, we assume the sub-Gaussianities for functional (or scalar) factors and idiosyncratic components. We relegate the definitions of sub-Gaussian (functional) process and multivariate (functional) linear process to Section E.3 of the Supplementary Material.

Assumption 4. For model (1), (i) $\{\mathbf{f}_t(\cdot)\}_{t \in [n]}$ and $\{\varepsilon_t(\cdot)\}_{t \in [n]}$ follow sub-Gaussian functional linear processes; (ii) $\mathcal{M}_\varepsilon < \infty$ and $\mathcal{M}_\varepsilon^2 \log p = o(n)$.

Assumption 4'. For model (2), (i) $\{\gamma_t\}_{t \in [n]}$ follows sub-Gaussian linear process and $\{\varepsilon_t(\cdot)\}_{t \in [n]}$ follows sub-Gaussian functional linear process; (ii) $\mathcal{M}_\varepsilon < \infty$ and $\mathcal{M}_\varepsilon^2 \log p = o(n)$.

Assumption 5. There exists some constant $\tau > 0$ such that $\min_{i, j \in [p]} \|\text{Var}(\varepsilon_{ti} \varepsilon_{tj})\|_{\mathcal{S}} \geq \tau$.

Assumption 6. The pair (n, p) satisfies $\mathcal{M}_\varepsilon^2 \log p = o(n/\log n)$ and $n = o(p^2)$.

Assumption 5 is required when implementing AFT, however, it is weaker than the similar assumption $\inf_{(u, v) \in \mathcal{U}^2} \min_{i, j \in [p]} \text{Var}[\varepsilon_{ti}(u) \varepsilon_{tj}(v)] \geq \tau$ imposed in Fang et al. (2023). Assumption 6 allows the high-dimensional case, where p grows exponentially as n increases.

3.2 Convergence of estimated loadings and factors

While the main focus of this paper is to estimate Σ_y , the estimation of factors and loadings remains a crucial aspect, encompassed by DIGIT and FPOET estimators, as well as in many other applications. We first present various convergence rates of estimated factors and loading matrix when implementing DIGIT. For the sake of simplicity, we denote

$$\varpi_{n,p} = \mathcal{M}_\varepsilon \sqrt{\log p/n} + 1/\sqrt{p}.$$

Theorem 1. *Suppose that Assumptions 1-4 hold. Then there exists an orthogonal matrix $\mathbf{U} \in \mathbb{R}^{r \times r}$ such that (i) $\|\widehat{\mathbf{B}} - \mathbf{B}\mathbf{U}^\top\|_{\max} = O_p(\varpi_{n,p})$; (ii) $n^{-1} \sum_{t=1}^n \|\widehat{\mathbf{f}}_t - \mathbf{U}\mathbf{f}_t\|^2 = O_p(\mathcal{M}_\varepsilon^2/n + 1/p)$; (iii) $\max_{t \in [n]} \|\widehat{\mathbf{f}}_t - \mathbf{U}\mathbf{f}_t\| = O_p(\mathcal{M}_\varepsilon \sqrt{\log n/n} + \sqrt{n^{1/2}/p})$.*

The orthogonal matrix \mathbf{U} above is needed to ensure that $\mathbf{b}_j^\top \widehat{\mathbf{b}}_j \geq 0$ for each $j \in [r]$. Provided that $\widehat{\mathbf{B}}\mathbf{U}\mathbf{U}^\top \widehat{\mathbf{f}}_t = \widehat{\mathbf{B}}\widehat{\mathbf{f}}_t$, the estimation of the common components and Σ_y remain unaffected by the choice of \mathbf{U} . By Theorem 1, we can derive the following corollary, which provides the uniform convergence rate of the estimated common component. Let $\check{\mathbf{b}}_i$ and $\check{\check{\mathbf{b}}}_i$ denote the i -th rows of \mathbf{B} and $\widehat{\mathbf{B}}$, respectively.

Corollary 1. *Under the assumptions of Theorem 1, we have $\max_{i \in [p], t \in [n]} \|\check{\mathbf{b}}_i^\top \widehat{\mathbf{f}}_t - \check{\check{\mathbf{b}}}_i^\top \mathbf{f}_t\| = O_p(\varrho)$, where $\varrho = \mathcal{M}_\varepsilon \sqrt{\log n \log p/n} + \sqrt{n^{1/2}/p}$.*

In the context of FPOET estimation of factors and loadings, we require an additional asymptotically orthogonal matrix \mathbf{H} such that $\widehat{\gamma}_t$ is a valid estimator of $\mathbf{H}\gamma_t$. Differing from DIGIT, we follow Bai (2003) to construct \mathbf{H} in a deterministic form. Let $\mathbf{V} \in \mathbb{R}^{r \times r}$ denote the diagonal matrix of the first r largest eigenvalues of $\widehat{\Sigma}_y^S$ in a decreasing order. Define $\mathbf{H} = n^{-1} \mathbf{V}^{-1} \widehat{\Gamma}^\top \Gamma \int \mathbf{Q}(u)^\top \mathbf{Q}(u) du$. By Lemma B35 of the Supplementary Material, \mathbf{H} is asymptotically orthogonal such that $\mathbf{I}_r = \mathbf{H}^\top \mathbf{H} + o_p(1) = \mathbf{H}\mathbf{H}^\top + o_p(1)$.

Theorem 1'. *Suppose that Assumptions 1'-4' hold. (i) $n^{-1} \sum_{t=1}^n \|\widehat{\gamma}_t - \mathbf{H}\gamma_t\|^2 = O_p(\mathcal{M}_\varepsilon^2/n + 1/p)$; (ii) $\max_{t \in [n]} \|\widehat{\gamma}_t - \mathbf{H}\gamma_t\| = O_p(\mathcal{M}_\varepsilon/\sqrt{n} + \sqrt{n^{1/2}/p})$; (iii) $\max_{i \in [p]} \|\widehat{\mathbf{q}}_i - \mathbf{H}\mathbf{q}_i\| = O_p(\varpi_{n,p})$.*

Corollary 1'. *Under the assumptions of Theorem 1', we have $\max_{i \in [p], t \in [n]} \|\hat{\mathbf{q}}_i^T \hat{\boldsymbol{\gamma}}_t - \mathbf{q}_i^T \boldsymbol{\gamma}_t\| = O_p(\varrho)$, where ϱ is specified in Corollary 1.*

The convergence rates presented in Theorem 1 and Corollary 1 for model (1) are, respectively, consistent to those established in Bai (2003) and Fan et al. (2013) when $\mathcal{M}_\varepsilon = O(1)$. Additionally, the rates in Theorem 1' and Corollary 1' for model (2) align with those in Theorem 1 and Corollary 1. These uniform convergence rates are essential not only for estimating the FFMs but also for many subsequent high-dimensional learning tasks.

Theorem 2. *Under the assumptions of Theorems 1 and 1', we have (i) $\mathbb{P}(\hat{r}^D = r) \rightarrow 1$, and (ii) $\mathbb{P}(\hat{r}^F = r) \rightarrow 1$ as $n, p \rightarrow \infty$, where \hat{r}^D and \hat{r}^F are defined in (18) and (19), respectively.*

Remark 5. *With the aid of Theorem 2, our estimators explored in Sections 3.2 and 3.3 are asymptotically adaptive to r . To see this, consider, e.g., model (2), and let $\hat{\boldsymbol{\gamma}}_{t, \hat{r}}$ and $\hat{\mathbf{q}}_{i, \hat{r}}(\cdot)$ be constructed using \hat{r}^F estimated scalar factors and functional loadings. Then, for any constant $\tilde{c} > 0$, $\mathbb{P}(\varrho^{-1} \max_{i \in [p], t \in [n]} \|\hat{\mathbf{q}}_{i, \hat{r}}^T \hat{\boldsymbol{\gamma}}_{t, \hat{r}} - \mathbf{q}_i^T \boldsymbol{\gamma}_t\| > \tilde{c}) \leq \mathbb{P}(\varrho^{-1} \max_{i \in [p], t \in [n]} \|\hat{\mathbf{q}}_i^T \hat{\boldsymbol{\gamma}}_t - \mathbf{q}_i^T \boldsymbol{\gamma}_t\| > \tilde{c} | \hat{r}^F = r) + \mathbb{P}(\hat{r}^F \neq r)$, which, combined with Corollary 1', implies that $\max_{i \in [p], t \in [n]} \|\hat{\mathbf{q}}_{i, \hat{r}}^T \hat{\boldsymbol{\gamma}}_{t, \hat{r}} - \mathbf{q}_i^T \boldsymbol{\gamma}_t\| = O_p(\varrho)$. Similar arguments can be applied to other estimated quantities in Sections 3.2 and 3.3. Therefore, we assume that r is known in our asymptotic results.*

3.3 Convergence of estimated covariance matrix functions

Estimating the idiosyncratic covariance matrix function $\boldsymbol{\Sigma}_\varepsilon$ is important in factor modeling and subsequent learning tasks. With the help of functional sparsity as specified in (7), we can obtain consistent estimators of $\boldsymbol{\Sigma}_\varepsilon$ under functional matrix ℓ_1 norm $\|\cdot\|_{S,1}$ in the high-dimensional scenario. The following rates of convergence based on estimated idiosyncratic components are consistent with the rate based on direct observations of independent functional data (Fang et al., 2023) when $\mathcal{M}_\varepsilon = O(1)$ and $p \log p \gtrsim n$.

Theorem 3. *Suppose that Assumptions 1–6 hold. Then, for a sufficiently large constant \dot{C} in (10), $\|\hat{\boldsymbol{\Sigma}}_\varepsilon^A - \boldsymbol{\Sigma}_\varepsilon\|_{S,1} = O_p(\varpi_{n,p}^{1-q} s_p)$.*

Theorem 3'. *Suppose that Assumptions 1'-4', 5, 6 hold. Then, for a sufficiently large constant \dot{C} in (10), $\|\widehat{\mathbf{R}}^A - \boldsymbol{\Sigma}_\varepsilon\|_{\mathcal{S},1} = O_p(\varpi_{n,p}^{1-q} s_p)$.*

When assessing the convergence criteria for our DIGIT and FPOET estimators, it is crucial to note that functional matrix norms such as $\|\cdot\|_{\mathcal{S},1}$ and $\|\cdot\|_{\mathcal{L}}$ are not suitable choices. This is because $\widehat{\boldsymbol{\Sigma}}_y$ may not converge to $\boldsymbol{\Sigma}_y$ in these norms for high-dimensional functional data, unless specific structural assumptions are directly imposed on $\boldsymbol{\Sigma}_y$. This issue does not arise from the poor performance of estimation methods but rather from the inherent limitation of high-dimensional models. To address this, we present convergence rates in functional elementwise ℓ_∞ norm $\|\cdot\|_{\mathcal{S},\max}$.

Theorem 4. *Under the assumptions of Theorem 3, we have $\|\widehat{\boldsymbol{\Sigma}}_y^{\mathcal{D}} - \boldsymbol{\Sigma}_y\|_{\mathcal{S},\max} = O_p(\varpi_{n,p})$.*

Theorem 4'. *Under the assumptions of Theorem 3', we have $\|\widehat{\boldsymbol{\Sigma}}_y^{\mathcal{F}} - \boldsymbol{\Sigma}_y\|_{\mathcal{S},\max} = O_p(\varpi_{n,p})$.*

Remark 6. (i) *The convergence rates of DIGIT and FPOET estimators (we use $\widehat{\boldsymbol{\Sigma}}_y$ to denote both) comprise two terms. The first term $O_p(\mathcal{M}_\varepsilon \sqrt{\log p/n})$ arises from the rate of $\widehat{\boldsymbol{\Sigma}}_y^{\mathcal{S}}$, while the second term $O_p(p^{-1/2})$ primarily stems from the estimation of unobservable factors. When $\mathcal{M}_\varepsilon = O(1)$, our rate aligns with the result obtained in [Fan et al. \(2013\)](#).*

(ii) *Compared to $\widehat{\boldsymbol{\Sigma}}_y^{\mathcal{S}}$, we observe that using a factor-guided approach results in the same rate in $\|\cdot\|_{\mathcal{S},\max}$ as long as $p \log p \gtrsim n$. Nevertheless, our proposed estimators offer several advantages. First, under a functional weighted quadratic norm introduced in [Section 4.1](#), which is closely related to functional risk management, $\widehat{\boldsymbol{\Sigma}}_y$ converges to $\boldsymbol{\Sigma}_y$ in the high-dimensional case (see [Theorem 6](#)), while $\widehat{\boldsymbol{\Sigma}}_y^{\mathcal{S}}$ does not achieve this convergence. Second, as evidenced by empirical results in [Sections 5 and 6](#), $\widehat{\boldsymbol{\Sigma}}_y$ significantly outperforms $\widehat{\boldsymbol{\Sigma}}_y^{\mathcal{S}}$ in terms of various functional matrix losses.*

Finally, we explore convergence properties of the inverse covariance matrix function estimation. Denote the null space of $\boldsymbol{\Sigma}_y$ and its orthogonal complement by $\ker(\boldsymbol{\Sigma}_y) = \{\mathbf{x} \in \mathbb{H}^p : \boldsymbol{\Sigma}_y(\mathbf{x}) = \mathbf{0}\}$ and $\ker(\boldsymbol{\Sigma}_y)^\perp = \{\mathbf{x} \in \mathbb{H}^p : \langle \mathbf{x}, \mathbf{y} \rangle = 0, \forall \mathbf{y} \in \ker(\boldsymbol{\Sigma}_y)\}$, respectively.

The inverse covariance matrix function Σ_y^{-1} corresponds to the inverse of the restricted covariance matrix function $\Sigma_y|_{\ker(\Sigma_y)^\perp}$, which restricts the domain of Σ_y to $\ker(\Sigma_y)^\perp$. The similar definition applies to the inverses of Σ_f and Σ_ε . With the DIGIT estimator $\widehat{\Sigma}_y^{\mathcal{D}}(\cdot, \cdot) = \widehat{\mathbf{B}}\widehat{\Sigma}_f(\cdot, \cdot)\widehat{\mathbf{B}}^\top + \widehat{\Sigma}_\varepsilon^{\mathcal{A}}(\cdot, \cdot)$, we apply Sherman–Morrison–Woodbury identity (Theorem 3.5.6 of [Hsing and Eubank, 2015](#)) to obtain its inverse $(\widehat{\Sigma}_y^{\mathcal{D}})^{-1} = (\widehat{\Sigma}_\varepsilon^{\mathcal{A}})^{-1} - (\widehat{\Sigma}_\varepsilon^{\mathcal{A}})^{-1}\widehat{\mathbf{B}}\{\widehat{\Sigma}_f^{-1} + \widehat{\mathbf{B}}^\top(\widehat{\Sigma}_\varepsilon^{\mathcal{A}})^{-1}\widehat{\mathbf{B}}\}^{-1}\widehat{\mathbf{B}}^\top(\widehat{\Sigma}_\varepsilon^{\mathcal{A}})^{-1}$. The inverse FPOET estimator can be obtained similarly. Then, within finite-dimensional Hilbert space, both the inverse DIGIT and FPOET estimators are consistent in the operator norm, as presented in the following theorems.

Theorem 5. *Suppose that the assumptions of Theorem 4 hold, $\varpi_{n,p}^{1-q}s_p = o(1)$, and both $\lambda_{\min}(\Sigma_\varepsilon)$ and $\lambda_{\min}(\Sigma_f)$ are bounded away from zero. Then, $\widehat{\Sigma}_y^{\mathcal{D}}$ has a bounded inverse with probability approaching 1, and $\|(\widehat{\Sigma}_y^{\mathcal{D}})^{-1} - \Sigma_y^{-1}\|_{\mathcal{L}} = O_p(\varpi_{n,p}^{1-q}s_p)$.*

Theorem 5'. *Suppose that the assumptions of Theorem 4' hold, $\varpi_{n,p}^{1-q}s_p = o(1)$, and $\lambda_{\min}(\Sigma_\varepsilon)$ is bounded away from zero. Then, $\widehat{\Sigma}_y^{\mathcal{F}}$ has a bounded inverse with probability approaching 1, and $\|(\widehat{\Sigma}_y^{\mathcal{F}})^{-1} - \Sigma_y^{-1}\|_{\mathcal{L}} = O_p(\varpi_{n,p}^{1-q}s_p)$.*

Remark 7. (i) *The condition that $\lambda_{\min}(\Sigma_\varepsilon)$ and $\lambda_{\min}(\Sigma_f)$ are bounded away from zero can also imply that $\lambda_{\min}(\Sigma_y)$ is bounded away from zero, which means that Σ_y has a finite number of nonzero eigenvalues, denoted as $d_n < \infty$, i.e., $\{\mathbf{y}_t(\cdot)\}_{t \in [n]}$ are finite-dimensional functional objects ([Bathia et al., 2010](#)). While the inverse of the sample covariance matrix function fails to exhibit convergence even though it operates within finite-dimensional Hilbert space, our factor-guided methods can achieve such convergence. It should be noted that d_n can be made arbitrarily large relative to n , e.g., $d_n = 2000, n = 200$. Hence, this finite-dimensional assumption does not place a practical constraint on our method. See also applications of inverse covariance matrix function estimation including functional risk management in Section 4.1 and sparse precision matrix function estimation in Section 4.2.*

(ii) *Within infinite-dimensional Hilbert space, Σ_y^{-1} becomes an unbounded operator, which is discontinuous and cannot be estimated in a meaningful way. However, Σ_y^{-1} is usually asso-*

ciated with another function/operator, and the composite function/operator in $\ker(\Sigma_y)^\perp$ can reasonably be assumed to be bounded, such as regression function/operator and discriminant direction function in Section 4.2. Specifically, consider the spectral decomposition (14), which is truncated at $d_n < \infty$, i.e., $\Sigma_{y,d_n}(u, v) = \sum_{i=1}^{d_n} \tau_i \varphi_i(u) \varphi_i(v)^\top$. Under certain smoothness conditions, such as those on coefficient functions in multivariate functional linear regression (Chiou et al., 2016), the impact of truncation errors through $\sum_{i=d_n+1}^{\infty} \tau_i^{-1} \varphi_i(u) \varphi_i(v)^\top$ on associated functions/operators is expected to diminish, ensuring the boundedness of composite functions/operators. Consequently, the primary focus shifts towards estimating the inverse of Σ_{y,d_n} , and our results in Theorems 5 and 5' become applicable.

Upon observation, a remarkable consistency is evident between DIGIT and FPOET methods developed under different models in terms of imposed regularity assumptions and associated convergence rates, despite the substantially different proof techniques employed.

4 Applications

4.1 Functional risk management

One main task of risk management in the stock market is to estimate the portfolio variance, which can be extended to the functional setting to account for additional intraday uncertainties. Consider a portfolio consisting of p stocks, where the i -th component of $\mathbf{y}_t(\cdot)$ represents the cumulative intraday return (CIDR) trajectory (Horváth et al., 2014) for the i -th stock on the t -th trading day. Additionally, let $\mathbf{w}(u) = \{w_1(u), \dots, w_p(u)\}^\top$ denote the allocation vector of the functional portfolio at time $u \in \mathcal{U}$. For a given $\mathbf{w}(\cdot)$, the true and perceived variances (i.e. risks) of the functional portfolio are $\langle \mathbf{w}, \Sigma_y(\mathbf{w}) \rangle$ and $\langle \mathbf{w}, \hat{\Sigma}_y(\mathbf{w}) \rangle$, respectively. According to Proposition S.1 of the Supplementary Material, the estimation error of the functional portfolio variance is bounded by

$$|\langle \mathbf{w}, \hat{\Sigma}_y(\mathbf{w}) \rangle - \langle \mathbf{w}, \Sigma_y(\mathbf{w}) \rangle| \leq \|\hat{\Sigma}_y - \Sigma_y\|_{\mathcal{S}, \max} \left(\sum_{i=1}^p \|w_i\| \right)^2,$$

in which Theorems 4 and 4' quantify the maximum approximation error $\|\widehat{\Sigma}_y - \Sigma_y\|_{\mathcal{S}, \max}$.

In addition to the absolute error between perceived and true risks, we are also interested in quantifying the relative error. To this end, we introduce the functional version of weighted quadratic norm (Fan et al., 2008), defined as $\|\mathbf{K}\|_{\mathcal{S}, \Sigma_y} = p^{-1/2} \|\Sigma_y^{-1/2} \mathbf{K} \Sigma_y^{-1/2}\|_{\mathcal{S}, \mathbb{F}}$, where $\mathbf{K} \in \mathbb{H}^p \otimes \mathbb{H}^p$ and the normalization factor $p^{-1/2}$ serves the role of $\|\Sigma_y\|_{\mathcal{S}, \Sigma_y} = 1$. To ensure the validity of this functional norm, we assume that Σ_y has a bounded inverse, which does not place a constraint in practice (see Remark 7(i)). With such functional norm, the relative error can be measured by

$$p^{-1/2} \|\Sigma_y^{-1/2} \widehat{\Sigma}_y \Sigma_y^{-1/2} - \tilde{\mathbf{I}}_p\|_{\mathcal{S}, \mathbb{F}} = \|\widehat{\Sigma}_y - \Sigma_y\|_{\mathcal{S}, \Sigma_y}, \quad (21)$$

where $\tilde{\mathbf{I}}_p$ denotes the identity operator. Provided that $\|\widehat{\Sigma}_y^{\mathcal{S}} - \Sigma_y\|_{\mathcal{S}, \Sigma_y} = O_p(\mathcal{M}_\varepsilon \sqrt{p/n})$, the sample covariance estimator fails to converge in $\|\cdot\|_{\mathcal{S}, \Sigma_y}$ under the high-dimensional setting with $p > n$. On the contrary, the following theorem reveals that our DIGIT estimator $\widehat{\Sigma}_y^{\mathcal{D}}$ converges to Σ_y as long as $\mathcal{M}_\varepsilon^4 p = o(n^2)$ and $\varpi_{n,p}^{1-q} s_p = o(1)$. The same result can also be extended to the FPOET estimator.

Theorem 6. *Under the assumptions of Theorem 5, we have $\|\widehat{\Sigma}_y^{\mathcal{D}} - \Sigma_y\|_{\mathcal{S}, \Sigma_y} = O_p(\mathcal{M}_\varepsilon^2 p^{1/2} n^{-1} + \varpi_{n,p}^{1-q} s_p)$.*

By Proposition S.2 of the Supplementary Material, the relative error is bounded by

$$|\langle \mathbf{w}, \widehat{\Sigma}_y(\mathbf{w}) \rangle / \langle \mathbf{w}, \Sigma_y(\mathbf{w}) \rangle - 1| \leq \|\Sigma_y^{-1/2} \widehat{\Sigma}_y \Sigma_y^{-1/2} - \tilde{\mathbf{I}}_p\|_{\mathcal{L}},$$

which, in conjunction with Theorem 6 and (21), controls the maximum relative error.

4.2 Estimation of precision matrix, regression, and discriminant direction functions

The second application considers estimating functional graphical models (Qiao et al., 2019), which aim to identify the conditional dependence structure among components in

$\mathbf{y}_t(\cdot)$. For Gaussian data, this task is equivalent to estimating the sparse inverse covariance (i.e., precision) matrix function, which is bounded for finite-dimensional functional objects. Our inverse DIGIT or FPOET estimators combined with functional thresholding can thus be utilized.

The third application explores multivariate functional linear regression (Chiou et al., 2016), which involves a scalar response z_t or a functional response

$$z_t(v) = \langle \mathbf{y}_t, \boldsymbol{\beta}(\cdot, v) \rangle + e_t(v), \quad v \in \mathcal{V},$$

where $\boldsymbol{\beta}(\cdot, \cdot) = \{\beta_1(\cdot, \cdot), \dots, \beta_p(\cdot, \cdot)\}^\top$ is operator-valued coefficient vector to be estimated. We can impose certain smoothness condition such that $\boldsymbol{\beta}(u, v) = \sum_{i=1}^{\infty} \tilde{\tau}_i \boldsymbol{\varphi}_i(u) \boldsymbol{\varphi}_i(v)^\top$ is sufficiently smooth relative to $\boldsymbol{\Sigma}_y(u, v) = \sum_{i=1}^{\infty} \tau_i \boldsymbol{\varphi}_i(u) \boldsymbol{\varphi}_i(v)^\top$, ensuring the boundedness of the regression operator $\boldsymbol{\beta}(u, v) = \int_{\mathcal{U}} \boldsymbol{\Sigma}_y^{-1}(u, u') \text{Cov}\{\mathbf{y}_t(u'), z_t(v)\} du'$. Replacing relevant terms by their (truncated) sample versions, we obtain $\hat{\boldsymbol{\beta}}(u, v) = n^{-1} \sum_{t=1}^n \int_{\mathcal{U}} \hat{\boldsymbol{\Sigma}}_{y, d_n}^{-1}(u, u') \mathbf{y}_t(u') z_t(v) du'$. This application highlights the need for estimators $\hat{\boldsymbol{\Sigma}}_{y, d_n}^{-1}$, as studied in Theorems 5 and 5'.

The fourth application delves into linear discriminant analysis for classifying multivariate functional data (Xue et al., 2023) with class labels $w_t = \{1, 2\}$. Specifically, we assume that $\mathbf{y}_t(\cdot)|w_t = 1$ and $\mathbf{y}_t(\cdot)|w_t = 2$ follow multivariate Gaussian distributions with mean functions $\boldsymbol{\mu}_1(\cdot)$ and $\boldsymbol{\mu}_2(\cdot)$, respectively, while sharing a common covariance matrix function $\boldsymbol{\Sigma}_y$. Our goal is to determine the linear classifier by estimating the discriminant direction function $\int_{\mathcal{U}} \boldsymbol{\Sigma}_y^{-1}(u, v) \{\boldsymbol{\mu}_1(v) - \boldsymbol{\mu}_2(v)\} dv$, which takes the same form as the regression function $\boldsymbol{\beta}(u) = \int_{\mathcal{U}} \boldsymbol{\Sigma}_y^{-1}(u, v) \text{Cov}\{\mathbf{y}_t(v), z_t\} dv$ encountered in the third application with a scalar response z_t . By similar arguments as above, both applications call for the use of estimators $\hat{\boldsymbol{\Sigma}}_{y, d_n}^{-1}$.

4.3 Estimation of correlation matrix function

The fifth application involves estimating the correlation matrix function and its inverse, which are essential in various graphical models for truly infinite-dimensional objects, see, e.g., Solea and Li (2022) and Zapata et al. (2022). Our proposed covariance estimators can

be employed to estimate the corresponding correlation matrix function and its inverse.

Specifically, let $\mathbf{D}_y(\cdot, \cdot) = \text{diag}\{\Sigma_{y,11}(\cdot, \cdot), \dots, \Sigma_{y,pp}(\cdot, \cdot)\}$ be the $p \times p$ diagonal matrix function. According to Baker (1973), there exists a correlation matrix function \mathbf{C}_y with $\|\mathbf{C}_y\|_{\mathcal{L}} \leq 1$ such that $\Sigma_y = \mathbf{D}_y^{1/2} \mathbf{C}_y \mathbf{D}_y^{1/2}$. Under certain compactness and smoothness assumptions, \mathbf{C}_y has a bounded inverse, denoted by Θ_y , and its functional sparsity pattern corresponds to the network (i.e., conditional dependence) structure among p components in $\mathbf{y}_t(\cdot)$; see Solea and Li (2022). In general, the estimator $\hat{\mathbf{D}}_y = \text{diag}(\hat{\Sigma}_{y,11}, \dots, \hat{\Sigma}_{y,pp})$ is non-invertible, so we can adopt the Tikhonov regularization to estimate \mathbf{C}_y by $\hat{\mathbf{C}}_y^{(\kappa)} = (\hat{\mathbf{D}}_y + \kappa \mathbf{I}_p)^{-1/2} \hat{\Sigma}_y (\hat{\mathbf{D}}_y + \kappa \mathbf{I}_p)^{-1/2}$ for some regularization parameter $\kappa > 0$. The estimator of Θ_y is then given by $\hat{\Theta}_y^{(\kappa)} = \hat{\mathbf{D}}_y^{1/2} (\hat{\Sigma}_y + \kappa \mathbf{I}_p)^{-1} \hat{\mathbf{D}}_y^{1/2}$. Consequently, we can plug into the DIGIT or the FPOET estimator for estimating \mathbf{C}_y and its inverse Θ_y .

5 Simulations

For the first data-generating process (denoted as DGP1), we generate observed data from model (1), where the entries of $\mathbf{B} \in \mathbb{R}^{p \times r}$ are sampled independently from $\text{Uniform}[-0.75, 0.75]$, satisfying Assumption 3(i). To mimic the infinite-dimensionality of functional data, each functional factor is generated by $f_{tj}(\cdot) = \sum_{i=1}^{50} \xi_{tji} \phi_i(\cdot)$ for $j \in [r]$ over $\mathcal{U} = [0, 1]$, where $\{\phi_i(\cdot)\}_{i=1}^{50}$ is a 50-dimensional Fourier basis and basis coefficients $\boldsymbol{\xi}_{ti} = (\xi_{t1i}, \dots, \xi_{tr i})^\top$ are generated from a vector autoregressive model, $\boldsymbol{\xi}_{ti} = \mathbf{A} \boldsymbol{\xi}_{t-1, i} + \mathbf{u}_{ti}$ with $\mathbf{A} = \{A_{jk} = 0.4^{|j-k|+1}\}_{r \times r}$, and the innovations $\{\mathbf{u}_{ti}\}_{t \in [n]}$ being sampled independently from $\mathcal{N}(\mathbf{0}_r, i^{-2} \mathbf{I}_r)$. For the second data-generating process (denoted as DGP2), we generate observed data from model (2), where r -vector of scalar factors $\boldsymbol{\gamma}_t$ is generated from a vector autoregressive model, $\boldsymbol{\gamma}_t = \mathbf{A} \boldsymbol{\gamma}_{t-1} + \mathbf{u}_t$ with $\{\mathbf{u}_t\}_{t \in [n]}$ being sampled independently from $\mathcal{N}(\mathbf{0}_r, \mathbf{I}_r)$. The functional loading matrix $\mathbf{Q}(\cdot) = \{Q_{jk}(\cdot)\}_{p \times r}$ is generated by $Q_{jk}(\cdot) = \sum_{i=1}^{50} i^{-1} q_{ijk} \phi_i(\cdot)$, where each q_{ijk} is sampled independently from the $\mathcal{N}(0, 0.3^2)$, satisfying Assumption 3'(i).

The idiosyncratic components are generated by $\boldsymbol{\varepsilon}_t(\cdot) = \sum_{l=1}^{25} 2^{-l/2} \boldsymbol{\psi}_{tl} \phi_l(\cdot)$, where each

ψ_{tl} is independently sampled from $\mathcal{N}(\mathbf{0}_p, \mathbf{C}_\zeta)$ with $\mathbf{C}_\zeta = \mathbf{D}\mathbf{C}_0\mathbf{D}$. Here, we set $\mathbf{D} = \text{diag}(D_1, \dots, D_p)$, where each D_i is generated from $\text{Gamma}(3, 1)$. The generation of \mathbf{C}_0 involves the following three steps: (i) we set the diagonal entries of $\check{\mathbf{C}}$ to 1, and generate the off-diagonal and symmetrical entries from $\text{Uniform}[0, 0.5]$; (ii) we employ hard thresholding (Cai and Liu, 2011) on $\check{\mathbf{C}}$ to obtain a sparse matrix $\check{\mathbf{C}}^\tau$, where the threshold level is found as the smallest value such that $\max_{i \in [p]} \sum_{j=1}^p I(\check{C}_{ij}^\tau \neq 0) \leq p^{1-\alpha}$ for $\alpha \in [0, 1]$; (iii) we set $\mathbf{C}_0 = \check{\mathbf{C}}^\tau + \tilde{\delta}\mathbf{I}_p$ where $\tilde{\delta} = \max\{-\lambda_{\min}(\check{\mathbf{C}}), 0\} + 0.01$ to guarantee the positive-definiteness of \mathbf{C}_0 . The parameter α controls the sparsity level with larger values yielding sparser structures in \mathbf{C}_0 as well as functional sparser patterns in $\Sigma_\varepsilon(\cdot, \cdot)$. This is implied from Proposition S.3(iii) of the Supplementary Material, whose parts (i) and (ii) respectively specify the true covariance matrix functions of $\mathbf{y}_t(\cdot)$ for DGP1 and DGP2.

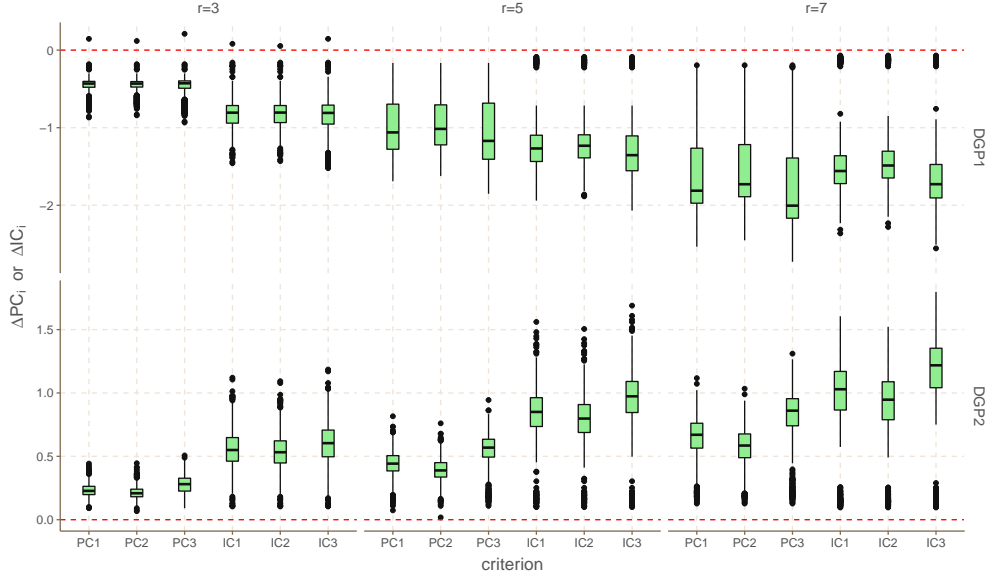


Figure 1: The boxplots of ΔPC_i and ΔIC_i ($i \in [3]$) for DGP1 and DGP2 with $p = 100, n = 100, \alpha = 0.5$, and $r = 3, 5, 7$ over 1000 simulation runs.

We firstly assess the finite-sample performance of the proposed information criteria in Section 2.4 under different combinations of p, n and α for DGP1 and DGP2. The results demonstrate that we can achieve almost 100% model selection accuracy in most cases. For instance, Figure 1 presents boxplots of ΔPC_i and ΔIC_i ($i = 1, 2, 3$) for two DGPs under

the setting $p = 100, n = 100, \alpha = 0.5$, and $r = 3, 5, 7$. See also similar results for $p = 200, n = 50, \alpha = 0.5$ in Figure S.1 of the Supplementary Material. We observe that, for DGP1 (or DGP2), nearly all values of ΔPC_i and ΔIC_i are less than (or greater than) zero, indicating that the observed data are more likely to be generated by the correct model (1) (or model (2)). Furthermore, different penalty functions $g(n, p)$ have similar impacts on the information criteria when p and n are relatively large.

Table 1: The average relative frequency estimates for $\mathbb{P}(\hat{r} = r)$ over 1000 simulation runs.

α	p	n	$r = 3$		$r = 5$		$r = 7$	
			$\mathbb{P}(\hat{r}^{\mathcal{D}} = r)$	$\mathbb{P}(\hat{r}^{\mathcal{F}} = r)$	$\mathbb{P}(\hat{r}^{\mathcal{D}} = r)$	$\mathbb{P}(\hat{r}^{\mathcal{F}} = r)$	$\mathbb{P}(\hat{r}^{\mathcal{D}} = r)$	$\mathbb{P}(\hat{r}^{\mathcal{F}} = r)$
0.25	100	100	0.854	0.828	0.762	0.715	0.618	0.597
		200	0.862	0.853	0.806	0.803	0.733	0.733
	200	100	0.922	0.868	0.832	0.792	0.739	0.667
		200	0.924	0.905	0.896	0.853	0.816	0.746
0.50	100	100	0.958	0.973	0.931	0.932	0.896	0.890
		200	0.960	0.974	0.952	0.950	0.936	0.943
	200	100	0.991	0.987	0.977	0.972	0.956	0.957
		200	0.991	0.993	0.984	0.985	0.979	0.971
0.75	100	100	0.990	0.998	0.986	0.991	0.979	0.976
		200	0.996	0.994	0.986	0.992	0.984	0.994
	200	100	0.997	1.000	0.998	1.000	0.995	0.999
		200	0.999	1.000	1.000	1.000	0.997	1.000

Once the more appropriate FFM is selected based on observed data, our next step adopts the ratio-based estimator (18) (or (19)) to determine the number of functional (or scalar) factors. The performance of proposed estimators is then examined in terms of their abilities to correctly identify the number of factors. Table 1 reports average relative frequencies $\hat{r} = r$ under different combinations of $r = 3, 5, 7, n = 100, 200, p = 100, 200$ and $\alpha = 0.25, 0.5, 0.75$ for both DGPs. Several conclusions can be drawn. First, for fixed p and n , larger values of α lead to improved accuracies in identifying r as the strength of factors (i.e. signal-to-noise

ratio, see Proposition S.3(iii) of the Supplementary Material) increases. Second, we observe the phenomenon of “blessing of dimensionality” in the sense that the estimation improves as p increases, which is due to the increased information from added components on the factors.

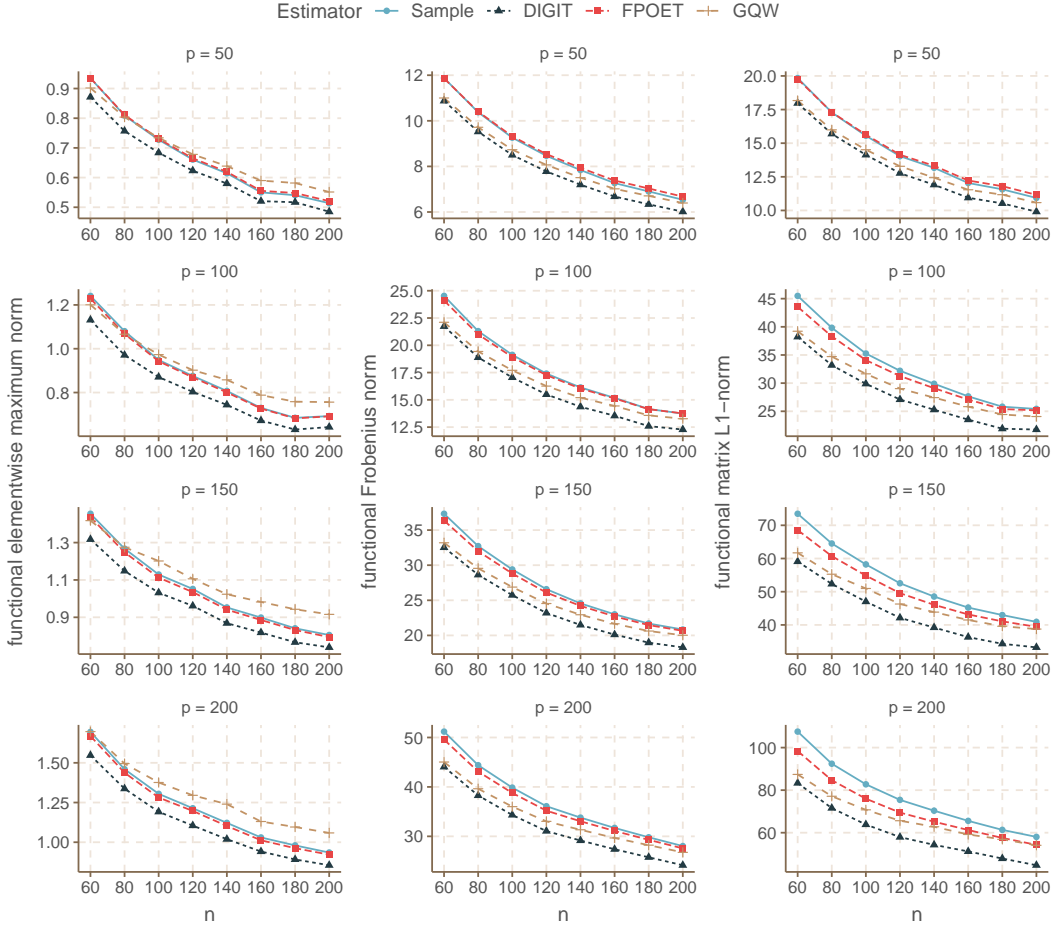


Figure 2: The average losses of $\hat{\Sigma}_y$ in functional elementwise ℓ_∞ norm (left column), Frobenius norm (middle column) and matrix ℓ_1 norm (right column) for DGP1 over 1000 simulation runs.

We next compare our proposed AFT estimator in (10) with two related methods for estimating the idiosyncratic covariance Σ_ε , where the details can be found in Section F of the Supplementary Material. Following Fan et al. (2013), the threshold level for AFT is selected as $\lambda = \hat{C}(\sqrt{\log p/n} + 1/\sqrt{p})$ with $\hat{C} = 0.5$. We also implemented the cross-validation method to choose \hat{C} . However, such method incurred heavy computational costs and only gave a very slight improvement. We finally compare our DIGIT and FPOET estimators

with two competing methods for estimating the covariance Σ_y . The first competitor is the sample covariance estimator $\hat{\Sigma}_y^S$. For comparison, we also implement the method of [Guo, Qiao and Wang \(2022\)](#) in conjunction with our AFT (denoted as GQW). This combined method firstly employs autocovariance-based eigenanalysis to estimate \mathbf{B} and then follows the similar procedure as DIGIT to estimate $\mathbf{f}_t(\cdot)$ and Σ_ε . Although DIGIT and GQW estimators (or FPOET estimator) are specifically developed to fit model (1) (or model (2)), we also use them (or it) for estimating Σ_y under DGP2 (or DGP1) to evaluate the robustness of each proposal under model misspecification. For both DGPs, we set $\alpha = 0.5$ and generate $n = 60, 80, \dots, 200$ observations of $p = 50, 100, 150, 200$ functional variables. We adopt the eigenvalue-ratio-based method to determine r . Figures 2 and 3 display the numerical summaries of losses measured by functional versions of elementwise ℓ_∞ norm, Frobenius norm, and matrix ℓ_1 norm for DGP1 and DGP2, respectively.

A few trends are observable. First, for DGP1 (or DGP2) in Figure 2 (or Figure 3), the DIGIT (or FPOET) estimator outperforms the three competitors under almost all functional matrix losses and settings we consider. In high-dimensional large p scenarios, the factor-guided estimators lead to more competitive performance, whereas the results of $\hat{\Sigma}_y^S$ severely deteriorate especially in terms of functional matrix ℓ_1 loss. Second, although both DIGIT and GQW estimators are developed to estimate model (1) and the idiosyncratic components are generated from a white noise process, our proposed DIGIT estimator is prominently superior to the GQW estimator for DGP1 under all scenarios, as seen in Figure 2. This demonstrates the advantage of covariance-based DIGIT over autocovariance-based GQW when the factors are pervasive (i.e. strong), however, DIGIT may not perform well in the presence of weak factors. Third, the FPOET estimator exhibits enhanced robustness compared to DIGIT and GQW estimators in the case of model misspecification. In particular, for DGP2, DIGIT and GQW show substantial decline in performance measured by functional Frobenius and matrix ℓ_1 losses, while, for DGP1, FPOET still achieves reasonably good performance. This suggests a preference for FPOET over DIGIT when the model form cannot be determined

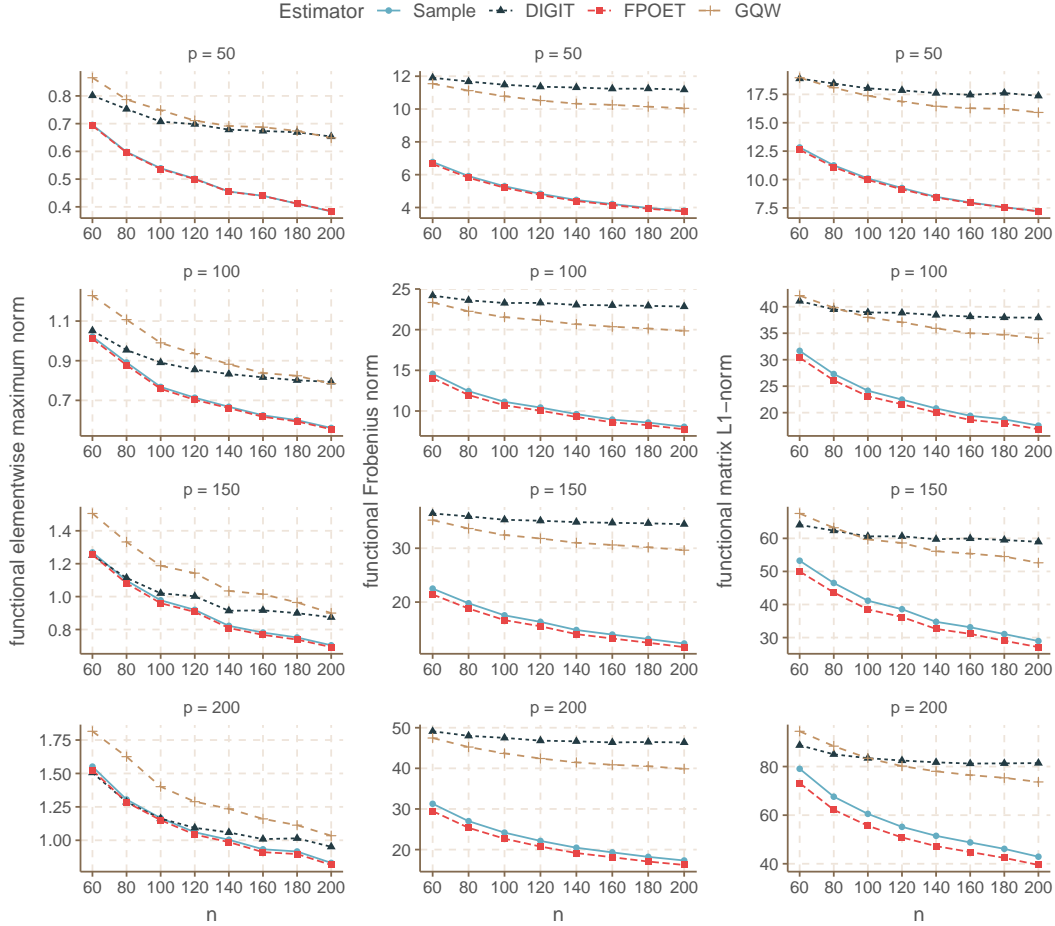


Figure 3: The average losses of $\hat{\Sigma}_y$ in functional elementwise ℓ_∞ norm (left column), Frobenius norm (middle column) and matrix ℓ_1 norm (right column) for DGP2 over 1000 simulation runs. confidently (i.e. information criteria between two FFMs are relatively close).

6 Real data analysis

6.1 Age-specific mortality data

Our first dataset, available at <https://www.mortality.org/>, contains age- and gender-specific mortality rates for $p = 32$ countries from 1960 to 2013 ($n = 54$). Following Tang et al. (2022) which also analyzed such dataset, we apply a log transformation to mortality rates and let $y_{ti}(u_k)$ ($t \in [n], i \in [p], k \in [101]$) be the log mortality rate of people aged $u_k = k - 1 \in \mathcal{U} =$

$[0, 100]$ living in the i -th country during the year $1959 + t$. The observed curves are smoothed based on a 10-dimensional B-spline basis. Figure S.9 of the Supplementary Material displays rainbow plots (Hyndman and Shang, 2010) of the smoothed log-mortality rates for females in six randomly selected countries, which use different colors to represent the curves from earlier years (in red) to more recent years (in purple). We observe a similar pattern for the USA, the U.K., and Austria, with their curves being more dispersed, indicating a uniform decline in mortality over time. However, this pattern differs significantly from those for Russia, Ukraine, and Belarus, where the decreasing effect disappears, and the curves are more concentrated. It is also worth mentioning that the U.K. and Austria are far from the USA, but Austria is closer to Russia, Ukraine, and Belarus. This phenomenon inspires us to employ multivariate functional time series methods, such as two FFMs, instead of spatial-temporal models that typically rely on geographical distance as the similarity measure.

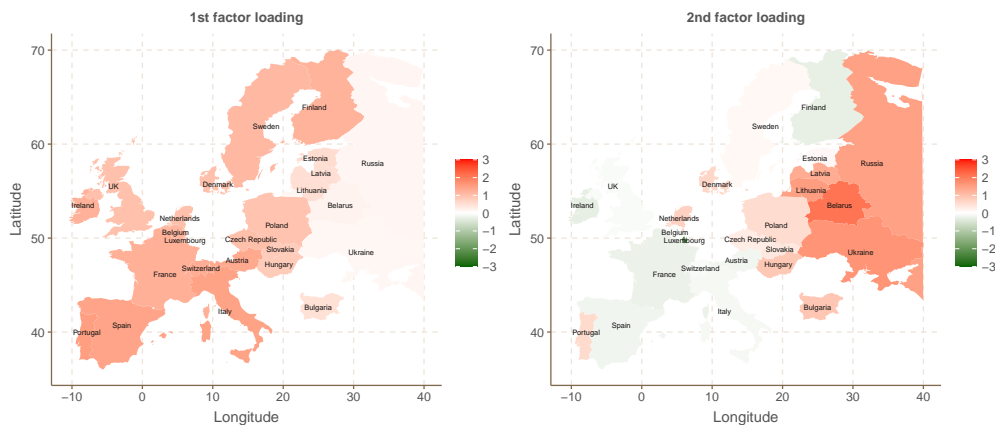


Figure 4: Spatial heatmaps of factor loadings of some European countries for females.

For model selection, we calculate the information criteria with $PC_1^D = 0.168 < PC_1^F = 0.177$, and $IC_1^D = -3.806 < IC_1^F = -3.448$. Therefore, we choose FFM (1) with age-specific factors for estimation. The leading two eigenvalues of $\hat{\Omega}$ in (8) are much larger than the rest with cumulative percentage exceeding 90%, so we choose $\hat{r}^D = 2$ for illustration. Figures 4 and S.10 of the Supplementary Material present spatial heatmaps of factor loading of some European countries for females and males, respectively. It is apparent that the first factor

mainly influences the regions of Western and Northern Europe, such as Italy, the U.K., Spain, and Sweden, while the former Soviet Union member countries such as Russia, Ukraine, Belarus, and Lithuania are heavily loaded regions on the second factor. Additionally, countries like Poland and Hungary that have experienced ideological shifts have non-negligible loadings on both factors. For countries far from Europe, such as the USA, Australia, and Japan, the first factor also serves as the main driving force.

Figures 5 and S.11 of the Supplementary Material provide the rainbow plots of the estimated age-specific factors for females and males, respectively. We observe that, for the first factor of female mortality rates, the curves of more recent years mostly lie below the curves of earlier years. This suggests a consistent improvement in mortality rates across all ages over the years. However, for the second factor, the curves of more recent years are located below the curves of earlier years when $u \leq 30$, and above them when $u > 30$, implying a downward trend under age 30 and an upward trend over age 30. Similar conclusions can be drawn for male mortality rates. By applying our factor-guided approach for multivariate functional time series, we achieve clustering results that are comparable to those obtained by Tang et al. (2022).

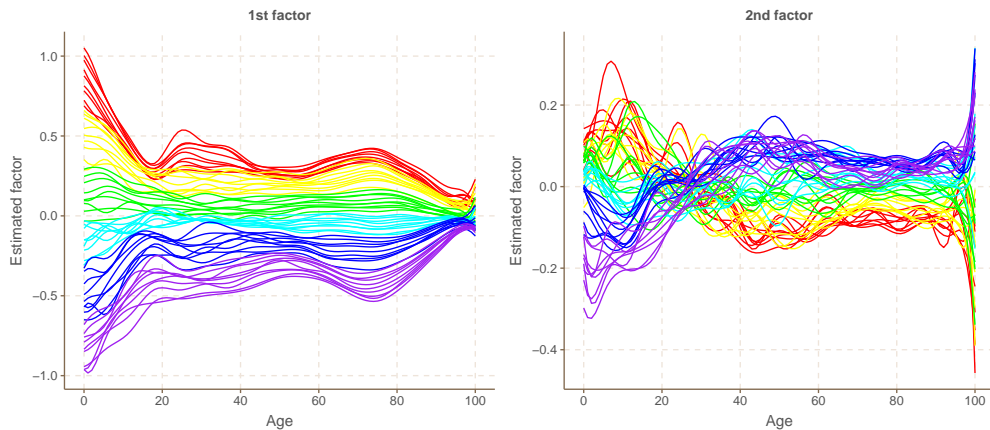


Figure 5: The estimated age-specific factors for females.

6.2 Cumulative intraday return data

Our second dataset, collected from <https://wrds-www.wharton.upenn.edu/>, consists of high-frequency observations of prices for a collection of S&P100 stocks from 251 trading days in the year 2017. We removed 2 stocks with missing data so $p = 98$ in our analysis. We obtain five-minute resolution prices by using the last transaction price in each five-minute interval after removing the outliers, and hence convert the trading period (9:30–16:00) to minutes $[0, 78]$. We construct CIDR (Horváth et al., 2014) trajectories, in percentage, by $y_{ti}(u_k) = 100[\log\{P_{ti}(u_k)\} - \log\{P_{ti}(u_1)\}]$, where $P_{ti}(u_k)$ ($t \in [n], i \in [p], k \in [78]$) denotes the price of the i -th stock at the k -th five-minute interval after the opening time on the t -th trading day. We obtain smoothed CIDR curves by expanding the data using a 10-dimensional B-spline basis. The CIDR curves, which always start from zero, not only have nearly the same shape as the original price curves but also enhance the plausibility of the stationarity assumption. We performed functional KPSS test (Horváth et al., 2014) for each stock, and found no overwhelming evidence (under 1% significance level) against the stationarity.

For model selection, the information criteria $PC_1^p = 0.567 > PC_1^f = 0.558$, and $IC_1^p = -0.619 > IC_1^f = -0.640$. These values suggest that FFM (2) is slightly more preferable and imply that the latent factors may not exhibit any intraday varying patterns. We consider the problem of functional risk management as discussed in Section 4.1. Our task is to obtain the optimal functional portfolio allocation $\hat{\mathbf{w}}(\cdot)$ by minimizing the perceived risk of the functional portfolio, specifically,

$$\hat{\mathbf{w}} = \arg \min_{\mathbf{w} \in \mathbb{H}^p} \langle \mathbf{w}, \hat{\Sigma}_y(\mathbf{w}) \rangle \quad \text{subject to} \quad \mathbf{w}(u)^T \mathbf{1}_p = 1 \text{ for any } u \in \mathcal{U},$$

where $\mathbf{1}_p = (1, \dots, 1)^T \in \mathbb{R}^p$. Following the derivations in Section E.4 of the Supplementary Material, we obtain the solution:

$$\hat{\mathbf{w}}(u) = \int \int \hat{\Sigma}_y^{-1}(u, v) \text{diag}\{H^{-1}(v, z), \dots, H^{-1}(v, z)\} \mathbf{1}_p dv dz$$

with $H(\cdot, \cdot) = \mathbf{1}_p^T \hat{\Sigma}_y^{-1}(\cdot, \cdot) \mathbf{1}_p$, which allows us to obtain the actual risk. In practical imple-

mentation, we treat components of $\mathbf{y}_t(\cdot)$ as finite-dimensional functional objects and hence can obtain bounded inverse $\widehat{\Sigma}_y^{-1}$ (and H^{-1}) using the leading eigenpairs of $\widehat{\Sigma}_y$ (and H) such that the corresponding cumulative percentage of selected eigenvalues exceeds 95%.

Table 2: Comparisons of the risks of functional portfolios obtained by using DIGIT, FPOET, GQW, and sample estimators.

Estimator	DIGIT			FPOET			GQW			Sample
	$\hat{r} = 1$	$\hat{r} = 2$	$\hat{r} = 3$	$\hat{r} = 1$	$\hat{r} = 2$	$\hat{r} = 3$	$\hat{r} = 1$	$\hat{r} = 2$	$\hat{r} = 3$	
July	0.052	0.060	0.058	0.057	0.060	0.057	0.083	0.062	0.052	0.099
August	0.044	0.045	0.048	0.045	0.044	0.049	0.050	0.089	0.085	0.092
September	0.092	0.051	0.065	0.093	0.053	0.058	0.108	0.056	0.060	0.097
October	0.077	0.045	0.042	0.079	0.044	0.041	0.082	0.067	0.051	0.086
November	0.078	0.060	0.043	0.079	0.063	0.045	0.063	0.073	0.076	0.090
December	0.075	0.075	0.043	0.077	0.079	0.042	0.083	0.079	0.095	0.091
Average	0.070	0.056	0.050	0.072	0.057	0.049	0.078	0.071	0.070	0.093

Following the procedure in [Fan et al. \(2013\)](#), on the 1st trading day of each month from July to December, we estimate $\widehat{\Sigma}_y$ using DIGIT, FPOET, GQW and sample estimators based on the historical data comprising CIDR curves of 98 stocks for the preceding 6 months ($n = 126$). We then determine the corresponding optimal portfolio allocation $\widehat{\mathbf{w}}(u_k)$ for $k \in [78]$. At the end of the month after 21 trading days, we compare actual risks calculated by $78^{-2} \sum_{k,k' \in [78]} \widehat{\mathbf{w}}(u_k)^\top \{21^{-1} \sum_{t=1}^{21} \mathbf{y}_t(u_k) \mathbf{y}_t(v_{k'})^\top\} \widehat{\mathbf{w}}(v_{k'})$. Following [Fan et al. \(2013\)](#) and [Wang et al. \(2021\)](#), we try $\hat{r} = 1, 2$ and 3 to check the effect of r in out-of-sample performance. The numerical results are summarized in [Table 2](#). We observe that the minimum risk functional portfolio created by DIGIT, FPOET, and GQW result in averaged risks over six months as 0.05, 0.049, and 0.07, respectively, while the sample covariance estimator gives 0.093. The risk has been significantly reduced by around 46% using our factor-guided approach.

References

- Bai, J. (2003). Inferential theory for factor models of large dimensions, *Econometrica* **71**: 135–171.
- Bai, J. and Ng, S. (2002). Determining the number of factors in approximate factor models, *Econometrica* **70**: 191–221.
- Baker, C. R. (1973). Joint measures and cross-covariance operators, *Transactions of the American Mathematical Society* **186**: 273–289.
- Bathia, N., Yao, Q. and Ziegelmann, F. (2010). Identifying the finite dimensionality of curve time series, *The Annals of Statistics* **38**: 3352–3386.
- Cai, T. and Liu, W. (2011). Adaptive thresholding for sparse covariance matrix estimation, *Journal of the American Statistical Association* **106**: 672–684.
- Carmeli, C., De Vito, E. and Toigo, A. (2006). Vector valued reproducing kernel Hilbert spaces of integrable functions and Mercer theorem, *Analysis and Applications* **4**: 377–408.
- Chiou, J.-M., Yang, Y.-F. and Chen, Y.-T. (2016). Multivariate functional linear regression and prediction, *Journal of Multivariate Analysis* **146**: 301–312.
- Fan, J., Fan, Y. and Lv, J. (2008). High dimensional covariance matrix estimation using a factor model, *Journal of Econometrics* **147**: 186–197.
- Fan, J. and Li, R. (2001). Variable selection via nonconcave penalized likelihood and its oracle properties, *Journal of the American Statistical Association* **96**: 1348–1360.
- Fan, J., Liao, Y. and Mincheva, M. (2013). Large covariance estimation by thresholding principal orthogonal complements, *Journal of the Royal Statistical Society: Series B* **75**: 603–680.
- Fan, J., Liu, H. and Wang, W. (2018). Large covariance estimation through elliptical factor models, *The Annals of Statistics* **46**: 1383.
- Fang, Q., Guo, S. and Qiao, X. (2023). Adaptive functional thresholding for sparse covariance function estimation in high dimensions, *Journal of the American Statistical Association*, *in press*.
- Guo, S. and Qiao, X. (2023). On consistency and sparsity for high-dimensional functional time series with application to autoregressions, *Bernoulli* **29**: 451–472.
- Guo, S., Qiao, X. and Wang, Q. (2022). Factor modelling for high-dimensional functional time series, *arXiv:2112.13651v2*.

- Hallin, M., Nisol, G. and Tavakoli, S. (2023). Factor models for high-dimensional functional time series I: Representation results, *Journal of Time Series Analysis, in press* .
- Happ, C. and Greven, S. (2018). Multivariate functional principal component analysis for data observed on different (dimensional) domains, *Journal of the American Statistical Association* **113**: 649–659.
- Horváth, L., Kokoszka, P. and Rice, G. (2014). Testing stationarity of functional time series, *Journal of Econometrics* **179**: 66–82.
- Hsing, T. and Eubank, R. (2015). *Theoretical Foundations of Functional Data Analysis, with an Introduction to Linear Operators*, John Wiley & Sons, Chichester.
- Hyndman, R. J. and Shang, H. L. (2010). Rainbow plots, bagplots, and boxplots for functional data, *Journal of Computational and Graphical Statistics* **19**: 29–45.
- Lam, C. and Yao, Q. (2012). Factor modelling for high-dimensional time series: Inference for the number of factors, *The Annals of Statistics* **40**: 694–726.
- Qiao, X., Guo, S. and James, G. (2019). Functional graphical models, *Journal of the American Statistical Association* **114**: 211–222.
- Solea, E. and Li, B. (2022). Copula gaussian graphical models for functional data, *Journal of the American Statistical Association* **117**: 781–793.
- Tang, C., Shang, H. L. and Yang, Y. (2022). Clustering and forecasting multiple functional time series, *The Annals of Applied Statistics* **16**: 2523–2553.
- Tavakoli, S., Nisol, G. and Hallin, M. (2023). Factor models for high-dimensional functional time series II: Estimation and forecasting, *Journal of Time Series Analysis, in press* .
- Wang, H., Peng, B., Li, D. and Leng, C. (2021). Nonparametric estimation of large covariance matrices with conditional sparsity, *Journal of Econometrics* **223**: 53–72.
- Wang, W. and Fan, J. (2017). Asymptotics of empirical eigenstructure for high dimensional spiked covariance, *The Annals of Statistics* **45**: 1342.
- Xue, K., Yang, J. and Yao, F. (2023). Optimal linear discriminant analysis for high-dimensional functional data, *Journal of the American Statistical Association, in press* .
- Zapata, J., Oh, S. Y. and Petersen, A. (2022). Partial separability and functional graphical models for multivariate Gaussian processes, *Biometrika* **109**: 665–681.
- Zou, H. (2006). The adaptive lasso and its oracle properties, *Journal of the American Statistical Association* **101**: 1418–1429.